Energy Conversion and Management: X 24 (2024) 100721

Contents lists available at ScienceDirect

Energy Conversion and Management: X

journal homepage: www.sciencedirect.com/journal/energy-conversion-and-management-x

Optimization and simulation of Tucuma and Ungurahui biodiesel process parameters and their effects on fuel properties

Arun Teja Doppalapudi [a,*], Abul Kalam Azad [a,*], M.M.K. Khan [b], Amanullah Maung Than Oo [c]

[a] School of Engineering and Technology, Central Queensland University, 120 Spencer Street, Melbourne, VIC 3000, Australia
[b] School of Engineering, Computer & Mathematical Sciences, Auckland University of Technology, Auckland, New Zealand
[c] School of Engineering, Macquarie University, Sydney, New South Wales, Australia

ARTICLE INFO

Keywords:
Biodiesel
Transesterification
Response surface methodology
Fuel properties
Process optimization
Aspen plus

ABSTRACT

The conversion parameters in biodiesel production have a substantial impact on the yield of methyl esters, consequently affecting the physicochemical properties of the fuel. Tucuma and Ungurahui bio-oils were used in this study to optimize the process parameters. A total of 27 transesterification experiments were conducted for each bio-oil, and the results were statistically investigated using the RSM approach. In addition, advanced kinetic modelling was performed using Aspen Plus software tools on the Tucuma biodiesel transesterification process to investigate the key effect of process parameters on the fuel properties. The study found a greater yield of 99.4 % and 99.5 % for Tucuma and Ungurahui, respectively, under optimized parametric conditions. ANOVA tests revealed lower *p*-values for catalyst and temperature, indicating their significant influence on the conversion process. For both fuels, GC–MS tests recorded 100 % methyl esters, and fuel properties agree with the ASTM biodiesel standards. Notably, the viscosity of both biodiesels is 4.0 mm^2/s, which closely matches that of diesel fuel. Furthermore, the process parameters such as methanol-to-oil ratio, catalyst, and temperatures influenced the methyl esters such as oleate, linoleate, and palmitate, impacting properties density and calorific value. Besides, viscosity was affected by the time parameter, which in turn influenced methyl stearate. The study concludes that while the process parameters influenced the fuel properties, their overall impact on the change was marginal.

1. Introduction

Fossil fuels are the primary energy sources, and 80 % of global energy is derived from fossil sources [1]. Especially fossil petroleum sources are contributing 33 % of total energy supply [2]. The major concern of using fossil fuel sources is the emission of large amounts of greenhouse gases, such as carbon monoxide (CO) and hydrocarbons (HC), which are primarily responsible for global warming. The World Energy Outlook 2023 (WEO 2023) reports that global energy-related CO_2 emissions peaked at 37 Gt CO_2 in 2022 [3]. Under the Net Zero Emissions (NZE) by 2050 Scenario (NZE Scenario), emissions need to be reduced to 24 Gt CO_2 by 2030, with the goal of reaching net zero by 2050 [3]. The transportation sector is one of the primary consumers of fossil fuels and stringent regulations are being implemented for automobiles to reduce emissions. Conventional fuels such as gasoline and diesel impact on the air quality and the increase in greenhouse gas emissions, which worsen climate change and present major public health hazards [4]. The transportation sector is a significant consumer of energy, as it is essential for economic development [5]. Alternative fuels such as biodiesel fuels can reduce the greenhouse gas emissions. For instance, converting one ton of algal biomass into biodiesel can cut off up to 1.83 tons of atmospheric CO_2 [6,7]. Hence the research framework aims to identify alternative energy sources beyond fossil fuels or to meet energy needs by converting between existing energy sources [8].

The current research trend is moving towards upcycling the biowastes for sustainable fuel production to meet the increasing energy demand [9]. For instance, Fig. 1(a) presents the biodiesel demand forecast from 2016 to 2028 as per the International Energy Agency (IEA). As per the forecast, demand for biofuels is projected to increase by 38 billion litres from 2023 to 2028, indicating a nearly 30 % growth compared to the previous five-year period [10]. While advanced economies like the European Union, the United States, Canada, and Japan are enhancing their transportation policies, the growth in volume is limited due to factors such as increased adoption of electric vehicles,

* Corresponding authors.
E-mail addresses: a.doppalapudi@cqu.edu.au (A.T. Doppalapudi), a.k.azad@cqu.edu.au (A.K. Azad).

https://doi.org/10.1016/j.ecmx.2024.100721
Received 29 July 2024; Received in revised form 1 September 2024; Accepted 17 September 2024
Available online 24 September 2024

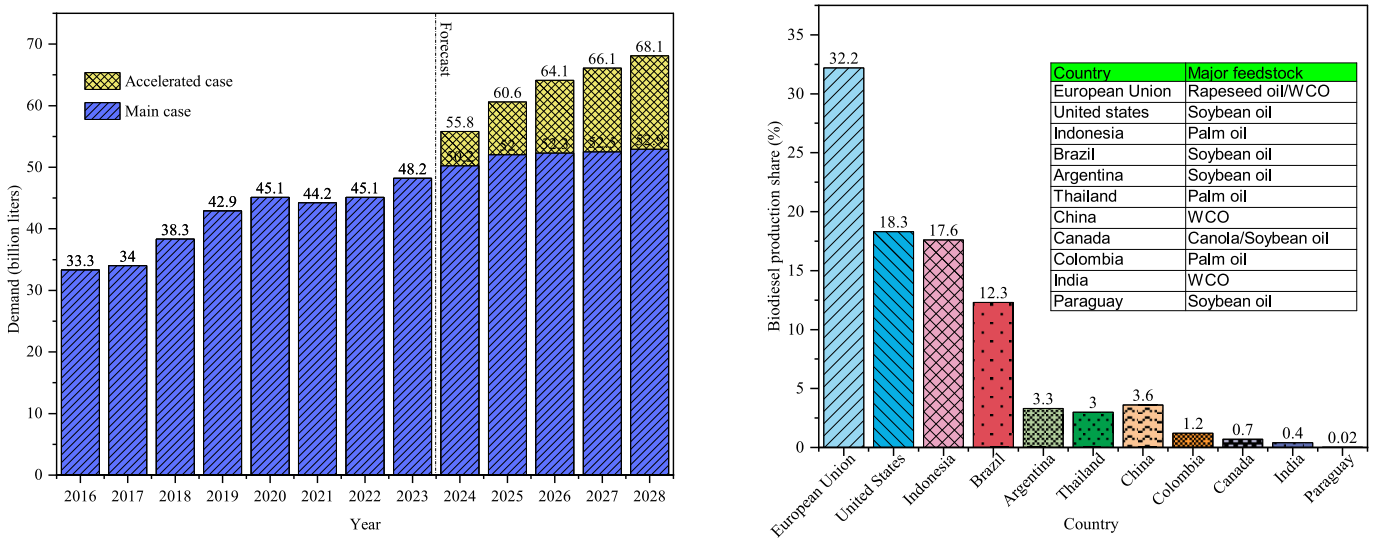

Fig. 1. Biodiesel demand and production; (a) biodiesel demand forecast from 2016 to 2028 [10]; (b) biodiesel production share by country and their primary feedstocks [18].

improvements in vehicle efficiency, high costs of biofuels, and technical constraints [11–13]. Renewable diesel and jet fuel are the main segments experiencing growth in these regions. The majority of new biofuel demand is emerging from developing economies, particularly Brazil, Indonesia, and India. These three nations have strong biofuel policies for increasing production values and maintaining ample potential for feedstock [14–16]. More research should be focussed on better yield conversion technologies and novel feedstocks to reduce the overall production costs of biodiesel.

The majority of the biodiesel production is from the edible oils. Currently, 70 % of the total biodiesel production is from vegetable oils (rapeseed oil accounting for 14 %, soybean oil for 23 %, and palm oil for 29 %) and non-edible waste cooking oils (WCO) contribute to the remaining 25 % of biodiesel production [17]. For example, Fig. 1(b) demonstrates the country-wise production share of biodiesel fuels and their primary feedstocks used in their respective countries. As per the OECD-FAO Agricultural Outlook 2023–2032, the European Union has produced 32.2 % of the total global biodiesel production, followed by the USA (18.3 %), Indonesia (17.6 %), and Brazil (12.3 %), respectively [18]. Moreover, the above-mentioned countries use rapeseed oil, soybean oil, palm oil, and other edible oils as primary feedstocks for biodiesel production. The utilisation of non-edible vegetable oils can still create significant opportunities for a more sustainable future.

Researchers are exploring potential non-edible sources across the countries to produce biodiesel to meet the required demands. For example, several wastes, such as rice husks [19], fruit peel wastes [20], animal manure [21], spent coffee grounds [22], and many more are being studied to produce biodiesel. One of the biggest challenges in biodiesel production is feedstock selection because the total cost of biodiesel conversion mainly depends on the feedstock type. Oils from different countries are assessed and reviewed for low-cost bio-oil production to narrow the choices for oil resources. This study reviewed over 150 feedstocks and has chosen, Tucuma and Ungurahui oils as the most prospective feedstocks, which are abundantly available in Latin American countries and northern regions of Brazil [23]. Tucuma and Ungurahui fatty esters are similar to the palm oil, with high palmitic and oleic content in its structure. As discussed, earlier palm oil has been widely used as a feedstock for the biodiesel conversion and considering the chemical structures of the Tucuma and Ungurahui, they can be used as the feedstocks instead of the palm oil. Despite its high nutritional value and beneficial properties, Tucuma oil is not used as a food ingredient or additive in the food industry. Besides, unsaturated fatty acids and carotenoids in Tucuma get easily oxidized, and the high free fatty acid content in the oil accelerates the initiation of oxidation reactions, which makes it unsuitable for consumption [24]. Similarly, Ungurahui oil is the 7th most abundant tree in the Amazon and also contains a high content of fatty acids [25–28]. Hence, both Tucuma and Ungurahui can be viable sources for biodiesel conversion. The fatty acid composition of Tucuma and Ungurahui is presented in the Supplementary materials. Very few studies were conducted on Tucuma biodiesel conversion process, where de Freitas et al. [29] has used spent battery as a catalyst and observed greater than 97 % conversion process. On the other hand, as per the authors understanding Ungurahui biodiesel conversion process has not been explored well and hence the study has chosen these two oils as the feedstocks for the biodiesel conversion process. As biodiesel is a mixture of fatty acid methyl esters, it can be converted through transesterification, supercritical fluid, thermal cracking pyrolysis, microemulsions, preheating oils, and many more [30].

Implementing biodiesel for commercial applications still needs to be refined due to technical and production factors [31–33]. Yield is an essential consideration to pursue in biodiesel conversion. The process variable compositions such as molar ratio, catalyst wt.%, reaction time, and temperature might create unreacted products during transesterification, ultimately affecting the yield [30]. These response variables can be evaluated efficiently through response surface methodology (RSM), artificial neural networks, Pareto-hierarchical framework, and other statistical procedures. The statistical analysis generated through these process parameters helps to evaluate the optimum product yield through graphical representations and regression analysis. The optimization of process variables for better yield supports large-scale applications [34]. Hence, the study has chosen an optimized conversion process for Tucuma and Ungurahui biodiesels that can suit large-scale applications. Moreover, another challenging aspect of using biodiesel applications in internal combustion engines is their variations in the physiochemical properties.

Biodiesel has higher density and viscosity and lower calorific value compared to diesel [35–37]. As mentioned earlier biodiesel is a mixture of methyl esters and these contents are similar in most biodiesel fuels but vary with the composition percentage [38,39]. The physical properties of biodiesel mainly depend on the methyl ester composition [40,41]. For instance, the presence of higher quantities of methyl oleate in the fuel blend has shown decreased fuel calorific value of the blend by 0.4 % [42]. Bukkarapu and Krishnasamy [42] observed a decrease in viscosity

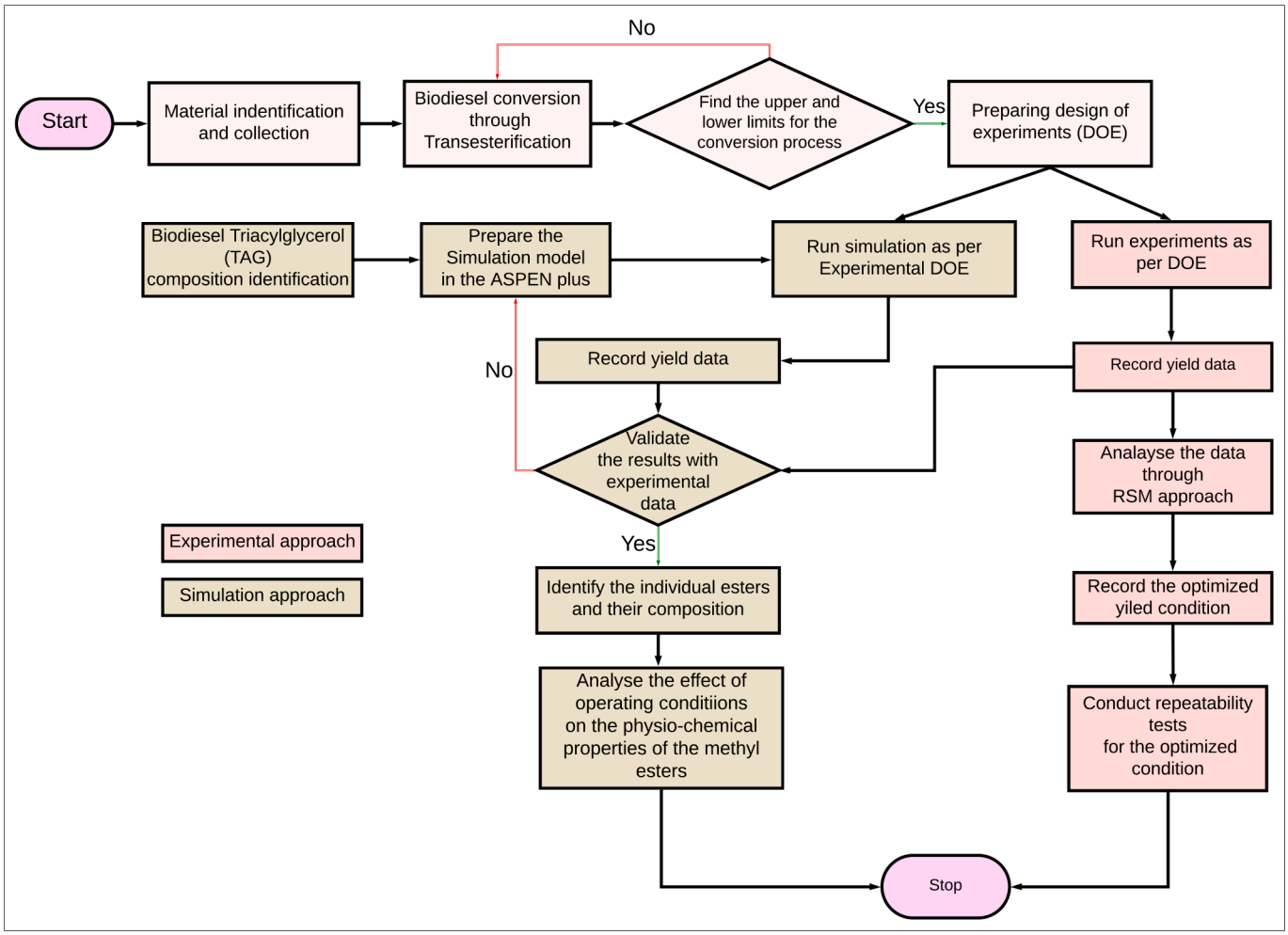

Fig. 2. Methodological approach for biodiesel conversion optimization and characterization of the fuel.

by 10.76 % with the addition of 20 % methyl myristate to the palm oil blend. Moreover, the higher quantities of methyl stearate in the biodiesel have shown increased viscosity of the fuels. The methyl ester composition cannot be changed; however, it can be observed from the literature that the fatty acid methyl esters (FAME) composition may vary with the varying operating conditions [43].

Simulation techniques are utilized in this study to analyze the variations of individual components and their impact on process parameters. Process simulation software, such as ASPEN Plus, Aspen Hysys, and BioSTEAM, is widely used for biodiesel conversion. Among these, ASPEN Plus and Aspen Hysys are particularly popular due to their advanced modeling capabilities. The built-in biodiesel components in the Aspen plus software database expedite property estimation and customizable modelling. Moreover, the software includes non-ideal thermodynamic models, such as Non-Random Two-Liquid (NRTL) and UNIFAC, which are essential for accurately simulating the transesterification reaction process.

From the literature, it is identified that biodiesel applications are effective in greenhouse gas emission reduction, and biodiesel feedstock plays a major role in determining the total cost of biodiesel production [44,45]. There are still a large number of potential feedstocks that are undiscovered and could be used for biodiesel production. Hence the study has chosen two new feedstocks Tucuma and Ungurahui, which can have a higher yield conversion rate. On the other hand, biodiesel's physiochemical properties pose a significant challenge in combustion aspects in IC engines [46]. The scope of this study includes investigating the biodiesel composition and how this composition varies with changes in biodiesel production parameters. There has been very limited research conducted on the biodiesel process variables and their effects on the physicochemical properties of the fuel. The study addresses this gap by conducting a complex simulation of the biodiesel conversion process. The novelty of the study is a simulation model for the transesterification process, created in Aspen Plus software with the tri-acyl glycerides (TAG) composition of Tucuma oil. The process parameters were varied using a statistical approach, and the individual effects on the physicochemical properties of the biodiesel were investigated. The aim of this study is to achieve a comprehensive understanding of how different production parameters affect the biodiesel's composition and properties. The following section presents the list of materials and methods used in this study to achieve the project goal.

2. Material and methods

2.1. Materials

Tucuma oil and Ungurahui oils are procured from market suppliers of the United States, Nature in Bottle. The mesocarp of Tucuma can carry 32.66 ± 1.2 % of oil [47], which contains 72 %–75 % unsaturated fatty acids and 25 %–28 % saturated fatty acids [23]. Whereas Ungurahui contains about 51 % fatty acids in its dry mesocarp [27]. In addition, methanol and high-grade potassium hydroxide (KOH) were obtained from Westlab Pty. Ltd., Australia, for the conversion reaction. The detailed methods for conversion, yield optimization, fuel testing, and other analyses are discussed in the following sections.

Table 1
Limits and levels of influencing biodiesel production parameters.

Independent variables	Levels		
	−1	0	1
Molar ratio (Methanol to oil ratio)	5:1	6:1	7:1
Catalyst wt.%	0.5	1.0	1.5
Reaction time (min)	50	60	70
Reaction temperature (°C)	50	60	70

2.2. Biodiesel fuel conversion method

Fig. 2 presents the methodology flow chart in this study to optimize the biodiesel conversion process and investigate the impact of biodiesel's physical properties on operating parameters. Firstly, design of experiments (DOE) was developed within the limits of operating parameters using the Box-Behnken statistical approach. The experimental procedure was then executed for each test, with the yield recorded as output responses. These responses were analysed using RSM to calculate the optimised yield conditions. Following this, a simulation study was conducted for Tucuma oil based on the prepared DOE, and the yield output was validated against experimental inputs. The individual methyl esters obtained in the simulation were examined with respect to the process parameters. The impacts of these process parameters on fuel's physiochemical properties were numerically investigated using a validated simulation model. Detailed methodological approaches for each test are reported in the subsequent sections.

2.2.1. Biodiesel conversion through transesterification

The transesterification reaction was performed to convert the Tucuma and Ungurahui fatty acids to their respective fatty acid methyl esters (FAME). The reaction was carried out in a round 3-neck flask with a reflux condenser using circulated cold water to condense the methanol vapors. Firstly, the flask was preheated to remove the water vapors, and a fixed amount of 100 mL (88.10 g for Tucuma and 90.40 g for Ungurahui) of bio-oil was added to the flask. Parallelly, as per DOE respective quantities of methanol and KOH catalyst were mixed rigorously in a closed conical flask to avoid the particle traces of the catalyst in the reaction. The methanol-KOH mixture is then mixed with the preheated bio-oil while maintaining the desired temperature within ±1°C. The mixture was agitated using the magnetic stirrer at 500 rpm. The reaction temperature, time, catalyst concentration, and methanol-oil molar ratio were followed as per the DOE list, as shown in Table 2. After the respective reaction periods, the obtained mixture was poured into the extraction funnel, providing eight hours for better separation of glycerol and FAME. The glycerol was decanted from the bottom of the separatory funnel, and the excess methanol, glycerol, and other products were then separated using demineralized water. The obtained methyl esters were heated at 110 °C for about 20 min to remove the water and excess methanol content in the obtained biodiesel.

1.1.1. Conversion optimization method (experimental)

The current study considered the Box–Behnken statistical method within the RSM to analyse the effects of independent process parameters. The DOE was created with four-factor variables such as molar ratio, catalyst wt.%, reaction time, and reaction temperature at three levels. Table 1 shows the three-level and 4-factor design matrix for the RSM approach. The independent variables were kept to three levels to determine the optimum point for higher yield.

The Box-Behnken approach was used for 27 experiments. The response (yield) generated from each reaction of these independent variables is expressed using the second-degree polynomial equations, as represented in Eq. (1) [48].

$$Y = \beta_0 + \sum_{j=1}^{k} \beta_j x_j + \sum_{ij=1}^{k} \beta_{ij} x_i x_j + \sum_{jj=1}^{k} \beta_{jj} x_j^2 + e \quad (1)$$

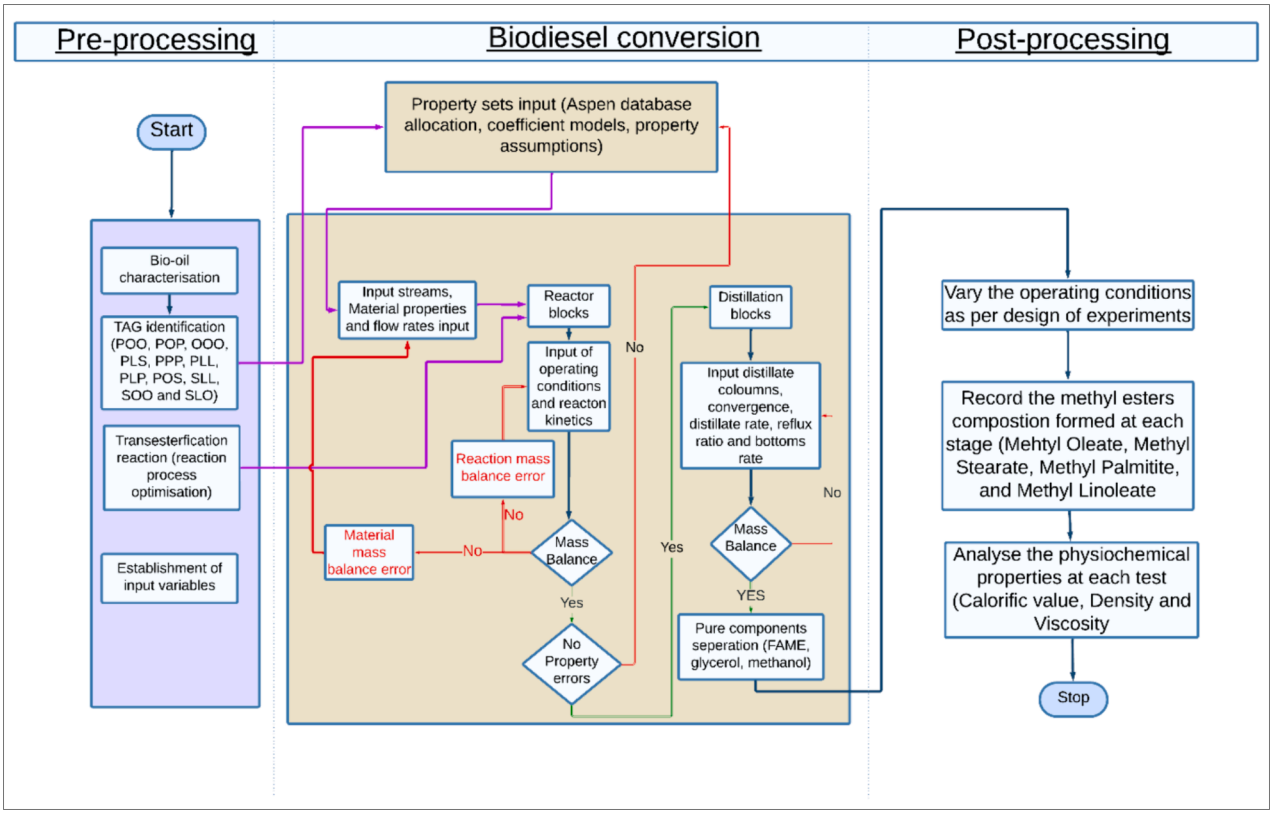

Fig. 3. Simulation approach of biodiesel conversion using the Aspen software.

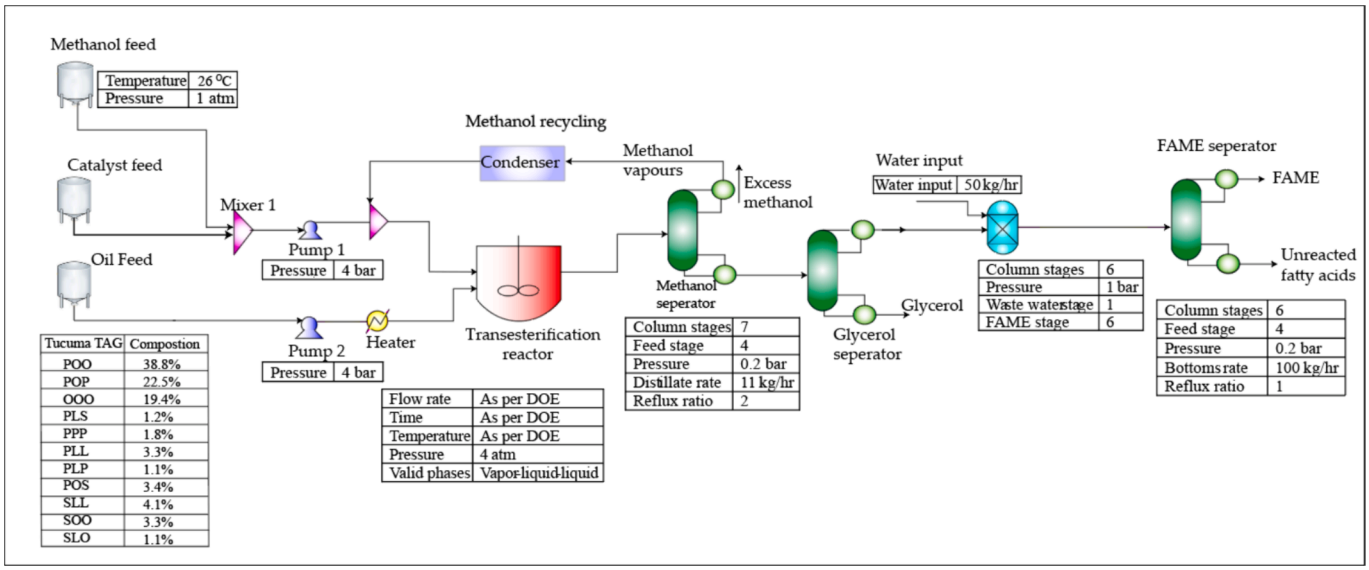

Fig. 4. Schematic diagram of Tucuma biodiesel conversion process in the Aspen Plus software.

where Y is the estimated yield of Tucuma FAME. xi and xj represent the process variables ranging from i to k, where k is the independent parameter that was investigated and optimized, which is 4 in this study. βj, βij, and βjj are the first-order, quadratic and linear coefficients for and between the i and j factors, and e refers to the experimental error assigned to Y [49–51].

2.2.2. FAME analysis and fuel properties test method

The analysis of FAME was performed according to AOCS Ce 1a-13 standards using gas chromatography-mass spectrometry (GC–MS) equipment. The GC column was operated at an oven temperature of 195 °C, utilizing split injection mode with an injection temperature of approximately 250 °C. The column dimensions were 30 m long, 0.32 mm in diameter, and 0.25 μm in thickness. The carrier gas pressure was maintained at 80.5 kPa, resulting in a total flow rate of 25 mL/min, while the column flow rate was set at 2.00 mL/min. During mass spectrometry analysis, the ion source temperatures were kept at 230 °C. The test samples were prepared by diluting them 1000 % using dichloromethane as the solvent. A total of 3 GC–MS tests were conducted for each fuel, and the average test results are presented in Table 4. The biodiesel yield was calculated using weight parameters as presented in Eq. (2) [52,53].

$$\text{Conversion yield} = \frac{\textit{Total weight of methyl ester}}{\textit{Total weight of oil in the sample}} \times 100 \qquad (2)$$

The prepared samples were tested as per the American society for testing materials (ASTM) standards. The density of the sample was measure as per ASTM D1298 standard at 15 °C and the viscosity of the samples were tested in RST Rheometer at 40 °C as per ASTM D445 standard. The calorific value was measured using a calorimeter with ASTM D240 test standards and the cetane index was calculated as per the ASTM D976 test standard. Similarly, the Cloud Point, Flash Point, Pour Point and acid values were tested as per ASTM D2500, ASTM D93/IP 34, ASTM D97/IP 15 and ASTM D664, respectively.

2.2.3. Biodiesel conversion modelling and simulation method

Fig. 3 illustrates the biodiesel simulation methodological approach in Aspen Plus software. Tucuma oil was used as the bio-oil in this simulation to analyse the effect of transesterification process parameters on the physio-chemical properties of biodiesel. The Aspen Plus database contains the individual components of triglycerides, diglycerides, and monoglycerides, which were used to create kinetic modelling reactions. Triacyl glycerol components were used as the input to the bio-oil, and as per the Teles et al. [54], the higher amounts of POO (38.8 %), POP (225 %), and OOO (19.4 %) were noticed in the oil, along with the smaller amounts of PLS (1.2 %), PPP (1.8 %), PLL (3.3 %), PLP (1.1 %), POS (3.4 %), SLL (4.1 %), SOO (3.3 %) and SLO (1.1 %).

The NRTL thermodynamic model was used with Aspen Plus software to simulate the conversion of biodiesel from triglycerides, involving KOH and methanol as essential components. The NRTL model was selected due to the presence of polar compounds (glycerol) and its straightforward approach to handling pseudo-components. The NRTL model is applied to determine both the activity coefficients and the binary interaction parameters [55]. NRTL performs well during methyl esters conversion as it accounts for non-ideal mixing behaviour. Moreover, NRTL deals with physical constraints, which is most suitable for the non-ideal conditions. As depicted in Fig. 4, methanol and KOH were mixed at room temperature (26 °C) under one atmospheric pressure conditions. Similarly, the oil was introduced into the reactor after being heated to 60 °C to ensure a consistent temperature distribution during transesterification. Tucuma oil mainly consists of oleic, palmitic, stearic, and linoleic components and traces of linolenic, myristic and arachidic acids.

The transesterification reaction was simulated using a Continuous Stirred-Tank Reactor (CSTR) model. The reactor operated by maintaining a pressure of 4 atm as recommended by Rabelo and Andrade [56]. The equilibrium kinetic reactions inside the reactor were where the activity in the vapour phase served as the basis, and the equilibrium constant was determined by estimating the Gibbs Free Energy [57]. The equilibrium reactions are presented in Eqs. (3)–(5) [58,59]. A total of 84 kinetic reactions were created to run the Tucuma oil transesterification. The list of components and the kinetic reactions are added in the Supplementary materials [60–62].

Table 2
DOE, experimental and prediction yield values for the optimized run orders.

Run Order	MeOH	Catalyst (Wt.%)	Temperature	Reaction time	Tucuma		Ungurahui	
					Experimental FAME conversion (%)	Predicted FAME conversion Fit (%)	Experimental FAME conversion (%)	Predicted FAME conversion Fit (%)
1	6	1	60	60	96.83	96.65	95.87	97.05
2	5	0.5	60	60	97.9	97.50	98.39	97.73
3	6	1	60	60	95.87	96.65	96.62	97.05
4	6	0.5	60	70	97.33	99.01	98.46	98.91
5	6	1.5	60	50	96.81	94.47	96.60	95.58
6	6	1	70	50	95.84	95.48	96.73	97.17
7	7	1.5	60	60	94.4	94.20	93.89	94.75
8	6	1.5	70	60	88.04	90.45	92.04	92.55
9	6	0.5	60	50	97.83	98.55	99.23	99.45
10	7	1	60	70	96.81	97.01	97.79	97.86
11	6	1	70	70	95.7	94.69	96.88	96.74
12	5	1	50	60	96.6	95.95	97.81	97.75
13	5	1	60	70	94.99	95.74	96.34	96.98
14	6	1.5	50	60	93.76	95.67	96.67	97.21
15	5	1	70	60	94.43	94.05	96.26	96.14
16	6	0.5	70	60	98.59	97.94	99.45	99.27
17	6	1	60	60	97.24	96.65	98.66	97.05
18	7	1	50	60	98.71	98.43	99.54	99.1
19	7	0.5	60	60	99.08	98.87	99.37	99.69
20	7	1	70	60	94.94	94.92	97.35	96.83
21	6	1	50	70	97.99	97.75	98.67	98.43
22	6	1.5	60	70	94.53	93.15	95.58	94.78
23	6	1	50	50	97.42	97.82	99	99.34
24	7	1	60	50	97.32	97.84	98.95	98.66
25	5	1	60	50	94.7	95.77	97.23	97.52
26	6	0.5	50	60	99.27	98.13	98.65	98.49
27	5	1.5	60	60	92.61	92.22	94.79	94.68

$$\underbrace{\text{Triglycerides}}_{\text{POO, POP, OOO.PLS, PPP, PLL,PLP, POS, SLL,SOO\&SLO}} + \text{Methanol} \overset{k_f,\, k_r}{\Leftrightarrow} \underbrace{\text{Diglycerides}}_{\text{PP,PO,OO,PS,OS,LS,LL,SS,PL,SL,SP\&OL}} + \underbrace{\text{Methyl esters}}_{\text{Oleate, Stearate, Palmitite \& Linoleate}} \tag{3}$$

$$\underbrace{\text{Diglycerides}}_{\text{PP,PO,OO,PS,OS,LS,LL,SS,PL,SL,SP\&OL}} + \text{Methanol} \overset{k_f,\, k_r}{\Leftrightarrow} \underbrace{\text{Monoglycerides}}_{\text{1–O , 1–P,1–L\&1–S}} + \underbrace{\text{Methyl esters}}_{\text{Oleate, Stearate,Palmitite \& Linoleate}} \tag{4}$$

$$\underbrace{\text{Monoglycerides}}_{\text{1–O, 1–P, 1–L\&1–S}} + \text{Methanol} \overset{k_f,\, k_r}{\Leftrightarrow} \underbrace{\text{Methyl esters}}_{\text{Oleate, Stearate, Palmitite \& Linoleate}} + \text{Glycerol} \tag{5}$$

where "k" denotes the rate constants for the elementary reactions and is defined by the Arrhenius equation as presented in Eq. (6) [63,56].

$$k = \alpha_{n,i} exp(\frac{A}{RT}) \tag{6}$$

where α is the frequency of the collisions, A is the activation energy, R is the gas constant, and T is the reaction mixture temperature.

According to the design of experiments, as outlined in Table 2, necessary adjustments were made to the flow rates of methanol, KOH, and oil, as well as reactor operating conditions, to conduct the reaction. During experimental conversion, a Liebig condenser was used to condense evaporated methanol from the reactor, which will then be returned to the reactor. However, in the simulation, methanol was recycled using a distillation column. In the case of simulation, the end products of the CSTR reactor contain methyl esters, unreacted free fatty acids (FFA), catalyst and methanol, which were then directed to a Methanol separator (RADFRAC model) to separate excess methanol at the top of the column.

The separated methanol was recycled, while the bottom stream was sent to another RADFRAC separator column to isolate the glycerol components. A mixture of fatty acid methyl esters (FAME) and triglycerides exiting in the glycerol separatory model was then subjected to water washing in a decanter model. The esters were subsequently washed in a decanter using water, where excess catalyst, glycerol, and water were collected at the end of the column, and the refined esters were sent to the distillation separator. In the FAME separation column was maintained at 120 °C to remove the water traces. The refined esters, which may contain traces of water, were further purified in the distillation separator. The mixture was heated to 140 °C to remove excess water in vapour form, and pure FAME was collected at the end of the distillation column. The bottom stream, containing fatty acids, which was recycled back to the oil feed, while purified FAME was recovered from the top stream.

3. Results and discussion

3.1. RSM-based optimisation

Table 2 presents the experimental and predicted biodiesel yields for the Tucuma and Ungurahui oil. A total of 27 experiments were generated to implement the box-Behnken experimental model with the help of

Table 3
Analysis of variance table for the optimized conditions of biodiesel.

Source	Tucuma						Ungurahui					
	DF	Adj SS	Adj MS	*f*-value	*p*-value	VIF	DF	Adj SS	Adj MS	*f*-value	*p*-value	VIF
Model	14	117.814	8.4153	3.70	0.014	1	14	76.8590	5.4899	6.98	0.001	
Linear	4	105.083	26.2707	11.54	0.000	1	4	63.6086	15.9021	20.21	0.000	1.00
MEOH	1	8.383	8.3834	3.68	0.079	1	1	3.0704	3.0704	3.90	0.072	1.00
Catalyst	1	74.252	74.2519	32.61	0.000	1	1	47.9200	47.9200	60.89	0.000	1.00
Temperature	1	21.897	21.8970	9.62	0.009		1	11.2714	11.2714	14.32	0.003	1.00
Time	1	0.550	0.5504	0.24	0.632	1.25	1	1.3467	1.3467	1.71	0.215	1.25
Square	4	4.570	1.1424	0.50	0.735	1.25	4	4.8018	1.2004	1.53	0.257	1.25
MEOH × MEOH	1	0.576	0.5764	0.25	0.624	1.25	1	0.0757	0.0757	0.10	0.762	1.25
Catalyst × Catalyst	1	2.058	2.0584	0.90	0.360	1.25	1	1.1021	1.1021	1.40	0.260	1.25
Temperature × Temp	1	1.222	1.2224	0.54	0.478		1	0.4383	0.4383	0.56	0.470	1.00
Time × Time	1	0.385	0.3852	0.17	0.688	1	1	1.8434	1.8434	2.34	0.152	1.00
2-Way Interaction	6	8.162	1.3603	0.60	0.728	1	6	8.4487	1.4081	1.79	0.184	1.00
MEOH × Catalyst	1	0.093	0.0930	0.04	0.843	1	1	0.8836	0.8836	1.12	0.310	1.00
MEOH × Temperature	1	0.640	0.6400	0.28	0.606	1	1	0.1024	0.1024	0.13	0.725	1.00
MEOH × Time	1	0.160	0.1600	0.07	0.795	1	1	0.0182	0.0182	0.02	0.882	1.00
Catalyst × Temperature	1	6.350	6.3504	2.79	0.121		1	7.3712	7.3712	9.37	0.010	
Catalyst × Time	1	0.792	0.7921	0.35	0.566		1	0.0156	0.0156	0.02	0.890	
Temperature × Time	1	0.126	0.1260	0.06	0.818		1	0.0576	0.0576	0.07	0.791	
Error	12	27.322	2.2769				12	9.4437	0.7870			
Lack-of-Fit	10	26.333	2.6333	5.33	0.168		10	5.2743	0.5274	0.25	0.946	
Pure Error	2	0.989	0.4944				2	4.1694	2.0847			
Total	26	145.136					26	86.3027				

coded levels. The optimal values are predicted in the software with respect to the condition.

3.2. Analysis of variance response (ANOVA) for the quadratic model

The regression equation model and the R^2 value of Tucuma and Ungurahui with 81.17 % and for 73.30 %, respectively suggest that the linear model fits well with the parameters. The full polynomial regression equation is presented in Eq. (7) for Tucuma and Eq. (8) for Ungurahui. The remaining variations cannot be elucidated by the model, which reflects the goodness of fit and confirms the adequacy of the regression model.

Model Summary for Tucuma				Model Summary for Ungurahui			
S	**R^2**	**R^2 (adj)**	**R^2 (pred)**	**S**	**R^2**	**R^2 (adj)**	**R^2 (pred)**
1.50893	81.17%	59.21%	0.00%	1565	73.70%	68.92%	61.04%

Regression Equation for Tucuma biodiesel yield = 37.5 + 8.1 MeOH + 18.6 catalyst + 1.04 temp − 0.03 time − 0.329 MeOH × MeOH − 2.48 catalyst × catalyst − 0.00479 temp × temp + 0.00269 time × time + 0.31 MeOH × catalyst − 0.0400 × temp − 0.0200 MeOH × time − 0.252 catalyst × temp − 0.089 catalyst × time − 0.00177 temp × time (7)

Regression equation for Ungurahui biodiesel = 113.2 + 1.38 MeOH + 22.32 catalyst − 0.145 temp − 0.758 time + 0.119 MeOH × MeOH − 1.82 catalyst × catalyst + 0.00287 temp × temp + 0.00588 time × time − 0.940 MeOH × catalyst − 0.0160 MeOH × temp − 0.0067 MeOH × time − 0.2715 catalyst × temp − 0.0125 catalyst × time + 0.00120 Temp × time (8)

The ANOVA depicts the influence of molar ratio, catalyst wt.%, reaction temperature, and time and their interaction. The current study has carried out confidence levels, an F-value test, the sum of squares (SS) and mean squares (MS) tests, and variance tests to assess the regression model's fitness. Table 3 presents the ANOVA findings for the methanol

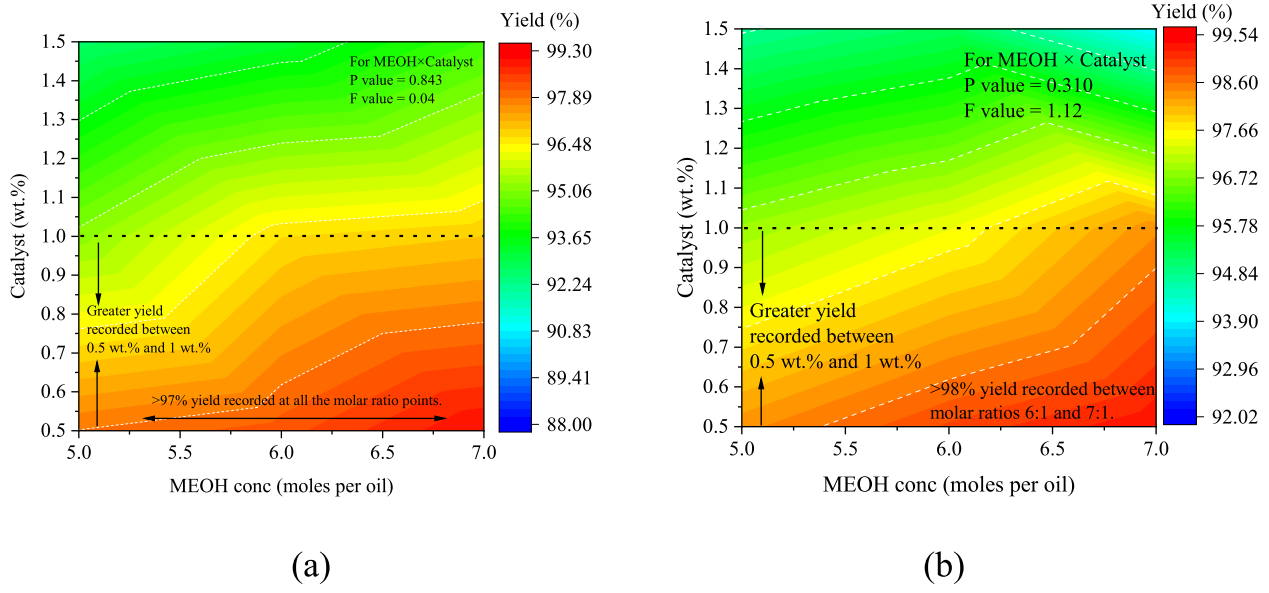

Fig. 5. Biodiesel yield influence with methanol to oil molar ratio and catalyst wt.%; (a) Tucuma (b) Ungurahui.

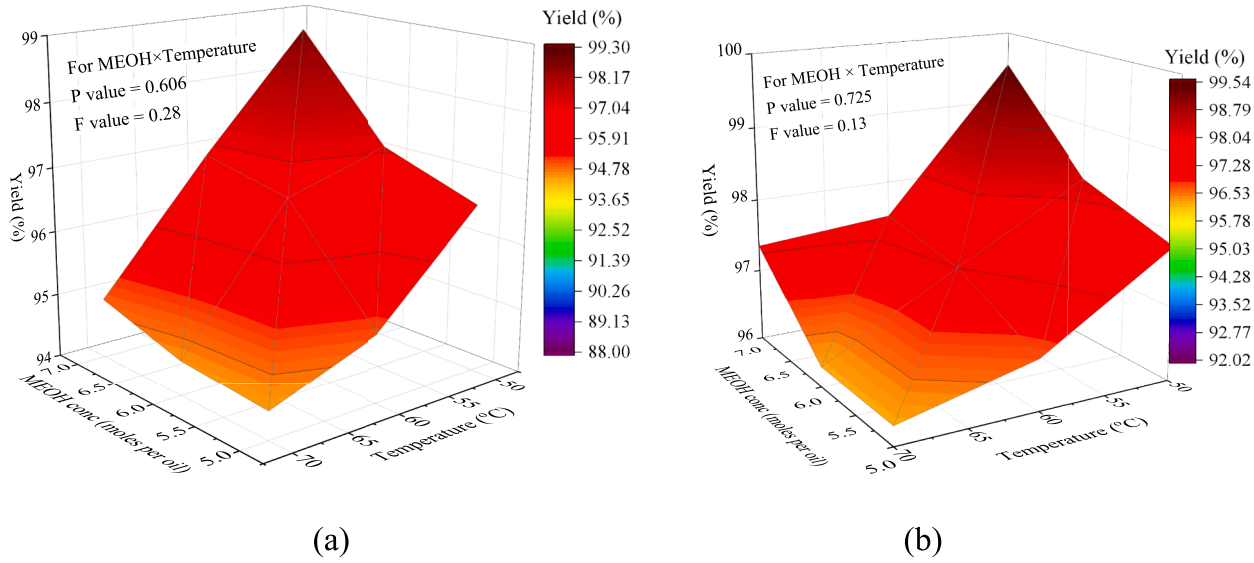

Fig. 6. Biodiesel yield influence with methanol to oil molar ratio and temperature: (a) Tucuma (b) Ungurahui.

molar ratio, catalyst, temperature, and time. The p-value is a probability that measures the evidence against the null hypothesis. Depicting from the P-value responses, catalyst, and time significantly influence the conversion process because the response values are less than 0.05. On the other hand, the molar ratio and residence time have less impact on the yield conversion process. The multicollinearity (VIF) value is 1, which clearly suggests that the regression analysis is good and that this analysis can proceed further.

Tucuma and Ungurahui models have the same degree of freedom (DF) 14. The Tucuma model is statistically significant but with a lower *f*-value (3.70) and a slightly higher *p*-value (0.014) compared to the Ungurahui model, with an *f*-value of 6.98 and a *p*-value of 0.001. Lack-of-Fit *p*-values for the Tucuma and Ungurahui are relatively high, suggesting that the presented models adequately fit the data. The lack of fit *p*-values for Tucuma model is 0.168. In contrast, the lack of fit *p*-vale of the Ungurahui is 0.946, indicating that Ungurahui model has a stronger overall fit to the data compared to Tucuma model. The total sum of squares (SS) value is higher for the Tucuma (145.13) compared to the Ungurahui (86.30), highlighting that the Tucuma model can exhibit more variability in the data set compared to the Ungurahui model.

3.3. Correlation of process parameters on yield conversion

The 2D contours and 3D surface plots were prepared to investigate the combined effect of multiple variables on the yield. The quadratic models were used to generate these graphs to understand the concurrent effect of the independent variables on biodiesel production. The effect of different parameters on conversion yield is presented in the following sections.

3.3.1. Effect of biodiesel yield: MeOH vs catalyst, time and temperature

Fig. 5 illustrates the effect of methanol and catalyst variations on the biodiesel conversion rates. To improve the rate of reaction, excess methanol is used in the transesterification process to promote the formation of methoxy species on the catalyst. However, higher methanol presence in the reaction above the optimal level will reduce the biodiesel yield [64]. Greater than 97 % yield is noted for both Tucuma and Ungurahui at the molar ratios 5:1, 6:1, and 7:1. However, a sharp

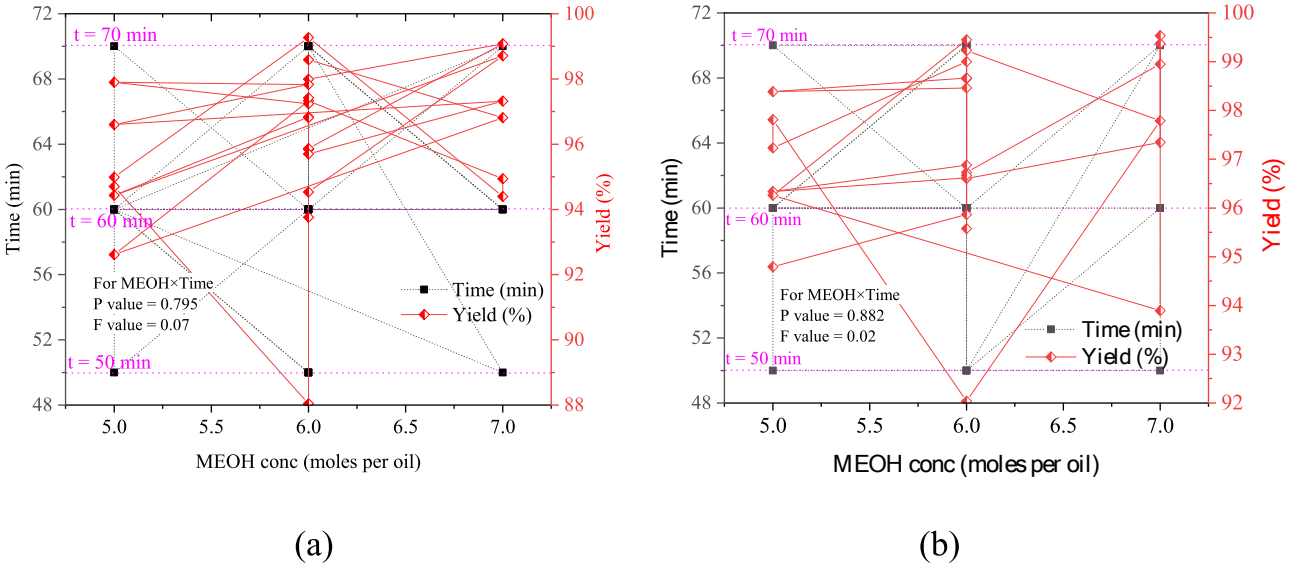

Fig. 7. Variation of yield with methanol to oil molar ratio and reaction time; (a) Tucuma (b) Ungurahui.

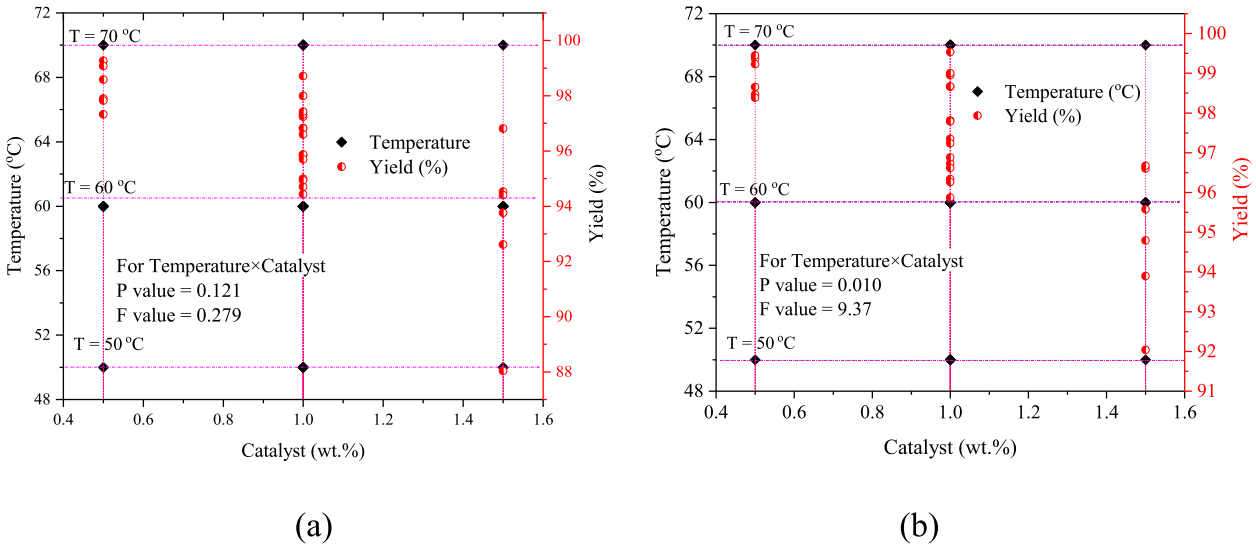

Fig. 8. Biodiesel yield influence with Temperature and catalyst wt.%; (a) Tucuma; (b) Ungurahui.

decrease in yield is noted with the increase in catalyst concentration [65]. From the responses from ANOVA Table 3, the *p*-value for the methanol is 0.079 for the Tucuma model and 0.072 for the Ungurahui model. Individual terms of methanol values indicate that the methanol has a marginal effect on the yield conversion rates. Whereas for the catalyst, the *p*-values are less than 0.05 for both the models, indicating that the catalyst has a significant effect on the biodiesel conversion rates. Hence, the effect of the catalyst is the dominating factor in this situation, where higher catalyst concentration reduces the biodiesel conversion yield even at a varying molar ratio of methanol. When the catalyst loading was increased to 1.5 by wt.%, the yield was decreased, and the triglycerides became more viscous to form soap [66]. The presence of higher concentrations of catalyst enhanced the formation the fatty acid salts (soap) [67]. Similar behaviour is also observed by Wong et al. [68]. In addition, the increase in catalyst to 1.5 % by weight has increased the viscosity of the product. The increased viscosity of the products reduces the mass transfer between the reactants and hinders the reaction rates, leading to lower yields of biodiesel [69]. Moreover, from the two-way interaction model of ANOVA between the methanol × catalyst aspect, the *p*-value is 0.310 and 0.01 for the Ungurahui and Tucuma models, respectively. There is a significant interaction effect between the methanol × catalyst parameters with the Tucuma model compared to Ungurahui model. This interaction can be clearly seen in Fig. 5, where higher variations in the yield scale values are noted with the Tucuma than with Ungurahui.

Fig. 6 presents the methanol molar ratio and temperature effect on the biodiesel yield process. At a high molar ratio and lower temperatures, a higher yield is observed. In general, a temperature rise improves the biodiesel yield, as the triglycerides get broken down and reduce the viscosity of the output. This will change the solubilities of the reactants and enhance the transfer rate of reactants to the products [70]. However, in this study, the increase in temperature has reduced the biodiesel yield. Temperature is the sensitive parameter in the transesterification process, as the slight increase in temperature can lead to significant differences in yield. The low temperatures helped the transesterification process by making the alcohol available throughout the process and enhancing the conversion rates [71]. With the temperature, the *f*-vales are higher, and *p*-values are lower. Hence, temperature has a significant effect on the conversion process. From the ANOVA, temperature shows a *p*-value of 0.009 for Tucuma and 0.003 for Ungurahui. The squared terms (methanol × methanol) and (temperature × temperature) and the two-way interaction term (methanol × temperature) are not significant in either model, as indicated by their high *p*-values. Though these terms may not have a significant impact on analysing the variability in the response variable, their presence in the model serves to explore higher-order effects and interactions.

Fig. 7 shows the effect of the reaction time and methanol molar ratio on the yield percentage. Depending on the molar ratio, at a longer reaction time, the yield is recorded as 96.4 %; however, at the same time, at a shorter reaction time near 50 min, a higher yield of 97.5 % is recorded. At shorter time intervals, base catalysts like KOH play a significant role in yield conversion [72]. Like Methanol, reaction time also showed a less significant effect on the yield conversion compared to temperature and catalyst. Though the 7:1 methanol to oil molar ratio showed a higher yield, and methanol might have less influence on the yield. On the other hand, excess methanol can lead to difficulties in the separation of glycerol [73–75]. From the statistical ANOVA analysis, both Tucuma and Ungurahui models exhibited non-significant interactions between methanol × time, highlighting that these parameters go along independently during yield conversion. Tucuma has a slightly higher *f*-value (0.07) compared to Ungurahui (0.02), indicating a marginally stronger but still non-significant interaction effect in Tucuma. The *p*-values for both Tucuma (0.795) and Ungurahui (0.882) are notably high, signifying a lack of statistical significance in the interaction between methanol and time for both fuel types. The findings suggest that changes in methanol concentration and time duration do not interact synergistically or antagonistically to significantly influence the yield of either Tucuma or Ungurahui within the tested experimental conditions. For instance, Boz et al. [76] varied the alcohol concentration from 6:1 to 18:1 and found no significant change to the yield percentage after the optimal 6:1 condition. Hence, the optimal operating conditions for maximizing yield in Tucuma and Ungurahui may be determined by factors other than Methanol and Time, such as Catalyst type and Temperature.

3.3.2. *Effect on biodiesel yield: catalyst vs temperature and time*

Fig. 8 presents the effect of temperature and catalyst wt.% on the biodiesel yield conversion for Tucuma and Ungurahui. As discussed earlier, the linear effect catalyst and the temperature in the biodiesel conversion process are high for Tucuma and Ungurahui. The higher range of biodiesel yield is noticed near low catalyst wt.% at varying temperatures. The sudden decrease in yield is noted with the increase in the catalyst by 1.5 wt%. A lower biodiesel yield, 88 %, is recorded at 1.5 wt% catalyst and at 70 °C. The heat energy used must be sufficient to overcome the diffusion resistance appearing in the three phases of the reaction mixture (i.e. oil-alcohol-catalyst). Similar results are also

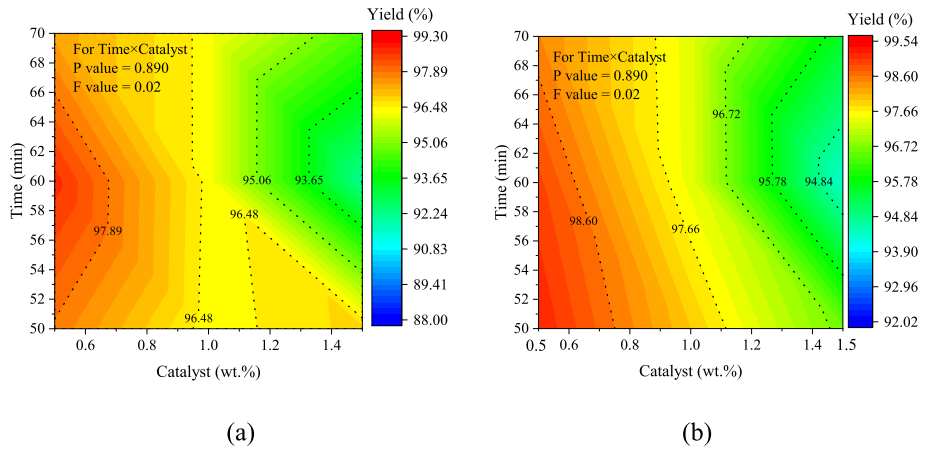

Fig. 9. Biodiesel yield influence with reaction time and catalyst wt.%; (a) Tucuma (b) Ungurahui.

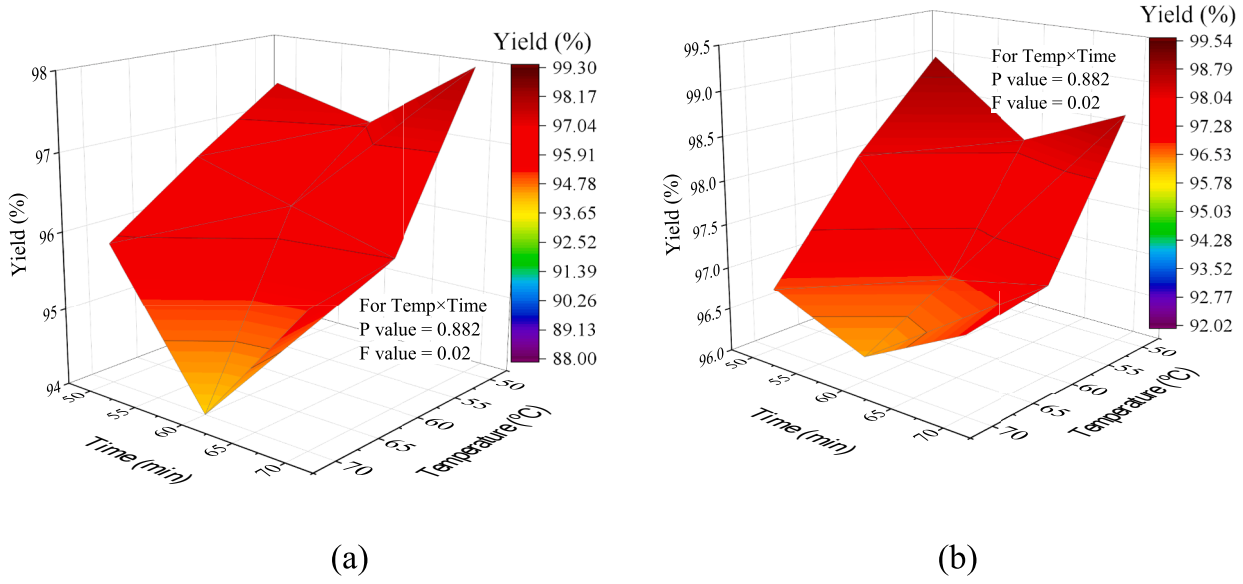

Fig. 10. Biodiesel yield influence with time and temperature; (a) Tucuma; (b) Ungurahui.

observed in the literature by Wu and Leung [77], Nautiyal et al. [78], and Leung et al. [79]. The linear effect of Temperature is significant for both Tucuma (p-value = 0.009) and Ungurahui (p-value = 0.003), indicating that changes in temperature influence the yield of these fuels. Using a temperature that exceeds the optimal range is not recommended because of the reversible nature of the reactions [80]. The increase in temperature effects the methyl esters and there by leads to formation of high-density triglycerides. Moreover, when the temperature reaches approximately the boiling point of methanol, it evaporates quickly and forms bubbles, complicating the reaction and decreasing biodiesel yield. For Tucuma, catalyst × temperature interaction is not statistically significant (p-value = 0.121), indicating that the combined effect of Catalyst type and Temperature does not strongly influence Tucuma yield under the tested conditions. However, with the Ungurahui model, catalyst × temperature interaction is significant (p-value = 0.010), indicating that variations in Catalyst type and Temperature together have a notable impact on Ungurahui yield. Future studies should concentrate on the analysis of varying the sensitivity ranges of these two factors will provide better understanding over the individual parameters and their effects on the conversion rates. The VIF values for both Tucuma and Ungurahui linear effects of Catalyst and Temperature are 1.00, indicating no multicollinearity issues among these predictor variables in the respective models.

Fig. 9 depicts the lower reaction time, and the lower catalyst concentration increases the yield. There are higher chances for producing more yield at 0.5 wt% catalyst and 60 min reaction time. A sharp decline in yield is noticed when the catalyst concertation is increased from 1.0 wt% to 1.5 wt%. In the Tucuma model, the interaction between catalyst × time is insignificant (p-value = 0.566), indicating that the combined effect of these factors does not strongly influence Tucuma yield. Similarly, in the Ungurahui model, the interaction between catalyst × time is also not significant (p-value = 0.890), suggesting a minimal impact of combined changes in Catalyst type and Time duration on Ungurahui yield. For Tucuma, the yield is increased till 60 min and then started decreasing rates with the increasing time. Similarly, for Ungurahui, at 50 min to 60 min time period higher yield is noted and the yield was decreased with the increasing time. This decrease in yield with the increase in time is due to the occurrence of reversible reactions, hence decrease in esters were noted [81].

3.3.3. *Effect of biodiesel yield: temperature vs time*

Fig. 10 demonstrates the effect of temperature and time on the yield percentage. It is observed that the temperature has a dominating impact on the yield % than the time. Higher reaction temperature increases

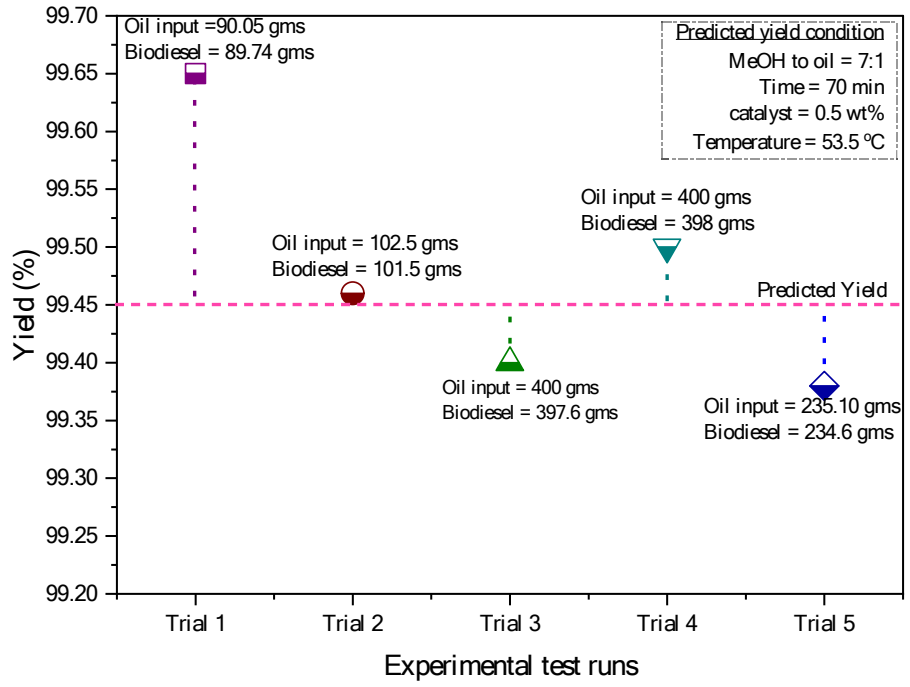

(a)

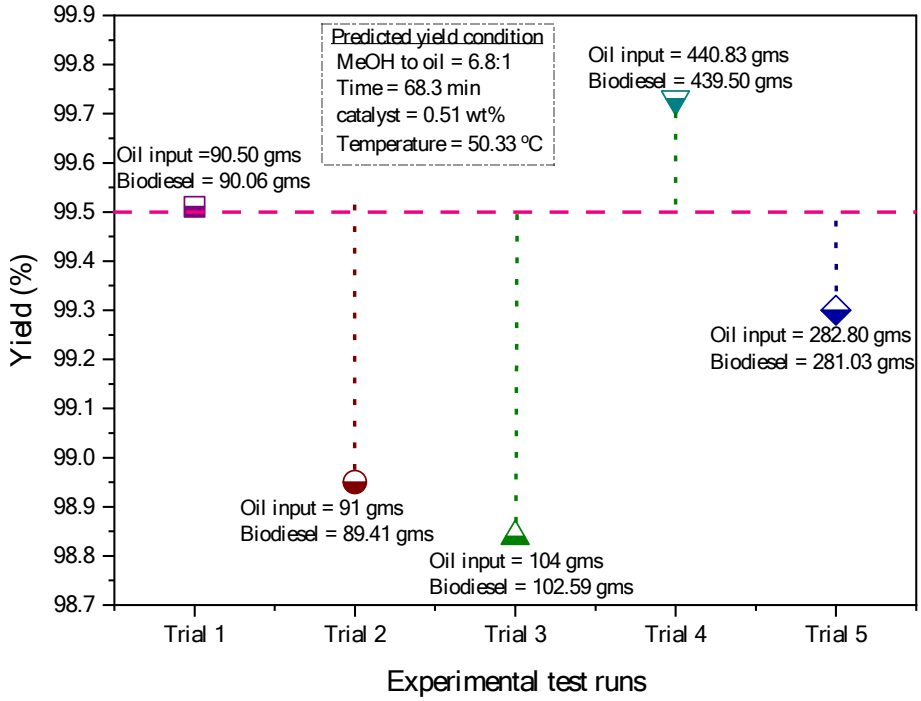

(b)

Fig. 11. Repeatability test results with predicted optimized yield; (a) Tucuma; (b) Ungurahui.

boiling point of the methanol and effects on the reaction rates [82]. However, raising the reaction temperature could lead to methanol loss, thereby slowing down the process. This would increase the free fatty acids (FFA) in the yield [83]. On the other hand, longer reaction duration will reduce the yield. In the initial stages of the biodiesel conversion process, the forward reaction was rapid until an equilibrium was reached [52]. However, the reverse reaction will begin after reactions that carry over the optimal time duration. Consequently, a longer-duration response reduces the yield of biodiesel [84]. Hence, determining the optimal reaction duration for transesterification is crucial, and in this study, the optimal reaction duration was 53 min with a 99.4 % biodiesel yield. At 50 °C, maximum ranges of biodiesel yield were

Table 4
FAME composition for Tucuma and Ungurahui biodiesels.

S. No	Methyl ester	Chemical name	Bonds	Tucuma biodiesel compositionAvg wt.% of 3 test results	Ungurahui biodiesel compositionAvg wt.% of 3 test results
1	Methyl oleate	$C_{19}H_{36}O_2$	Unsaturated	44.87	52.11
2	Methyl palmitate	$C_{17}H_{34}O_2$	Saturated	25.69	23.80
3	Methyl linoleate	$C_{19}H_{34}O_2$	Unsaturated	12.56	10.64
4	Methyl stearate	$C_{19}H_{38}O_2$	Saturated	11.79	9.60
5	Methyl Myristate	$C_{15}H_{30}O_2$	Saturated	1.72	0.56
6	Methyl Docosanoate	$C_{23}H_{46}O_2$	Saturated	1.02	1.72
7	Methyl arachidonate	$C_{21}H_{42}O_2$	Saturated	0.88	0.72
8	Methyl tetracosanoate	$C_{25}H_{50}O_2$	Saturated	0.35	0.37
9	Methyl Laureate	$C_{13}H_{26}O_2$	Saturated	0.33	–
10	Methyl margariate	$C_{18}H_{36}O_2$	saturated	0.18	–
11	Methyl eicosenoate	$C_{21}H_{40}O_2$	Unsaturated	0.17	0.21
12	Methyl palmoliate	$C_{17}H_{32}O_2$	Unsaturated	0.16	0.12
13	Methyl Methyl linolenate (9, 12, 15)	$C_{19}H_{32}O_2$	Unsaturated	0.16	0.15
14	Methyl linolenate (6,9, 12)	$C_{19}H_{32}O_2$	Unsaturated	0.10	–

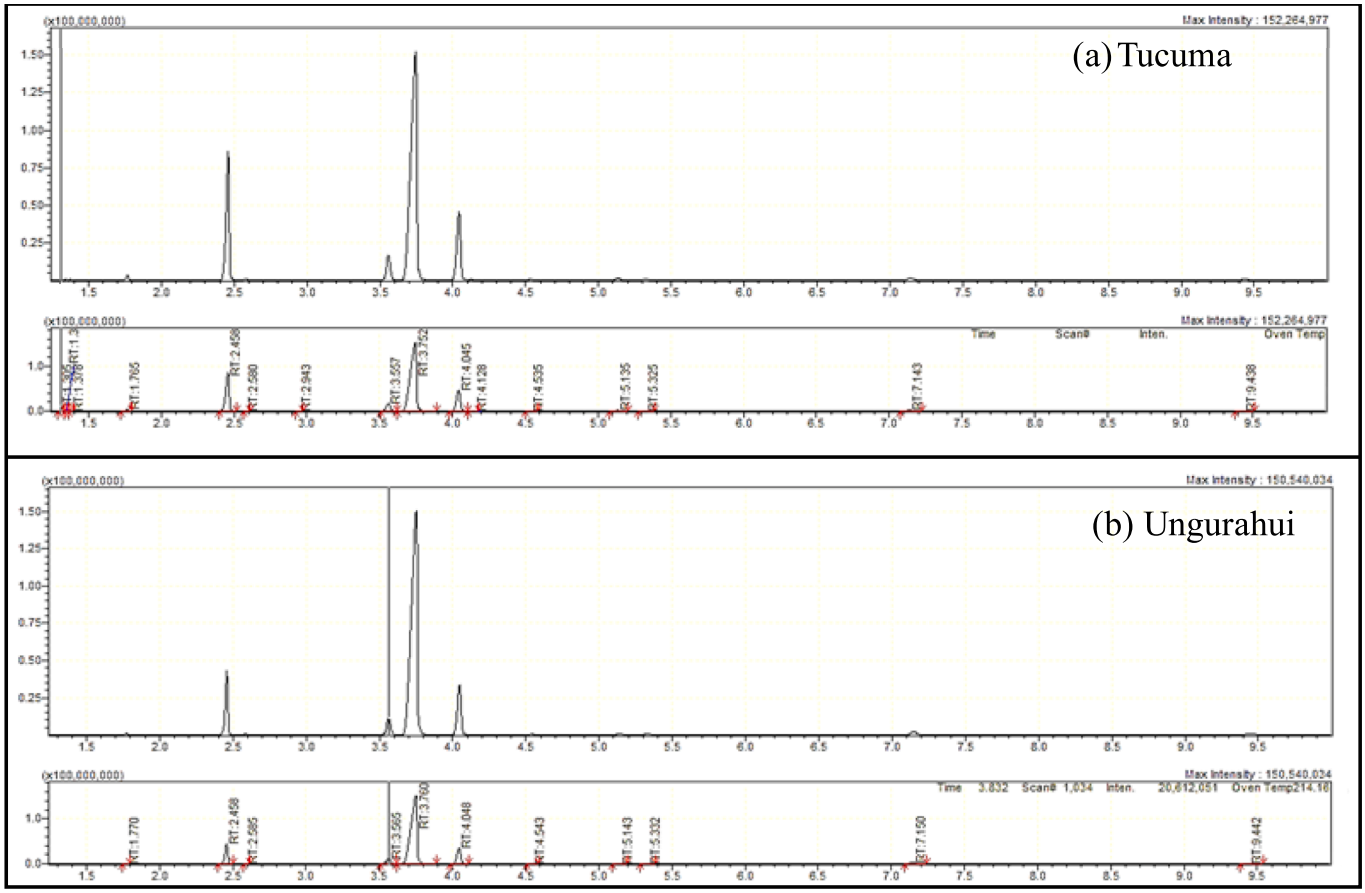

Fig. 12. Chromatogram of biodiesel; (a) Tucuma; (b) Ungurahui.

noted at varying reaction times. However, a significant decrease in yield is emphasized with the increase in temperature at all the reaction times [85]. This is because increase in reaction temperature and time causes the phase separation issues. The longer duration and high temperature reaction rates produces the triglycerides, making it more difficult to remove the glycerol and excess catalyst products, result in recovery of lower yield of biodiesel.

3.4. Optimization analysis

The regression equation is solved using the Minitab, and the optimum values for the parameters were predicted for the transesterification process of Tucuma and Ungurahui bio-oils. The optimized parameters to achieve 99.4 % condition are with the methanol-oil molar ratio of 7:1, catalyst concentration of 0.5 wt%, temperature of 53.5 °C and a period of 70 min. A total of 5 repeatability tests were conducted with different bio-oil weights at optimized conditions, and the yield results are in the range of 99.4 % ± 0.2 %, as shown in Fig. 11(a). Also, as shown in Fig. 11(b), the predicted yield to achieve 99.5 % condition was a methanol molar ratio of 6.8:1, catalyst concentration of 0.51 wt%, temperature of 50.33 °C, and a period of 68.3 min. The experimental repeatability tests recorded as 99.2 % ± 0.4 %, for the optimized condition of Ungurahui biodiesel. The fluctuations in the test results are attributed to system errors arising from the process, which involved the

Table 5
Physicochemical properties of Tucuma and Ungurahui biodiesel.

Property	Unit	Test Standard	ASTM D6751 standard biodiesel [94]	Tucuma biodiesel	Ungurahui biodiesel	Diesel [95]
Density at 15 °C	kg/m^3	ASTM D1298	860–890	879.1	880.3	832
Viscosity at 40 °C	mm^2/s	ASTM D445	1.9–6.0 mm^2/s	4.01	4.0	4.1
Calorific Value	MJ/kg	ASTM D240	–	39.87	39.82	45.7
Cetane Index		ASTM D976	Min^m 47	48.2	48.2	44
Cloud Point	°C	ASTM D2500	Min^m 100	8	4	8.6
Flash Point	°C	ASTM D93/IP 34	Report	185.9	176.5	62
Pour Point	°C	ASTM D97/IP 15	–	−6	−6	−15
Acid Number	mg KOH/g	ASTMD664	Max^m 0.5	0.47	0.56	–

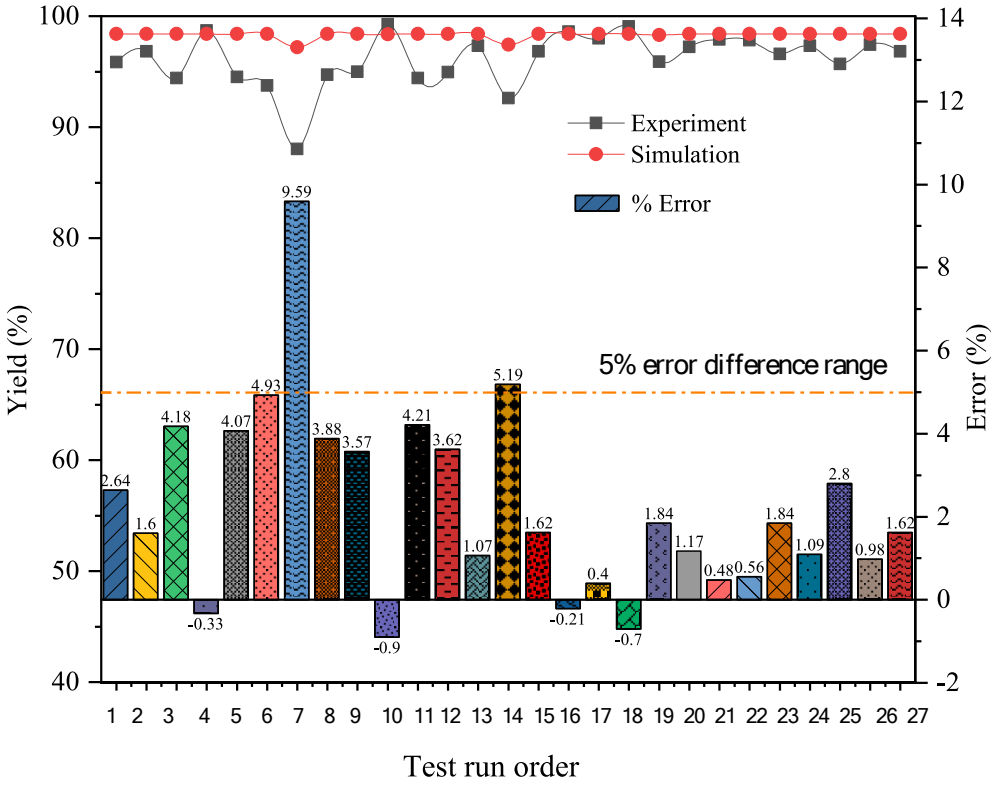

Fig. 13. Comparison of experimental yield with simulation yield.

transfer of fluids from one beaker to another. Given the similarity of the methyl esters for both Tucuma and Ungurahui, the optimized test conditions resulted in closer outcomes.

3.5. FAME analysis of Tucuma and Ungurahui biodiesel

The transesterification reaction converted the fatty acids to fatty acid esters through glycerol extraction. Table 4 presents the components of FAME, and Fig. 12 presents the chromatogram of Tucuma and Ungurahui biodiesel fuels, respectively.

For Tucuma, unsaturated fatty acid esters account for approximately 58 %, whereas saturated fatty acids account for 42 %. Meanwhile, for Ungurahui, unsaturated and saturated fatty acids account for 63 % and 36 %, respectively. With biodiesel, the fuel stability and combustion behaviour highly depend on the methyl ester composition [86]. For instance, improved oxidation stability was noticed with the saturated fatty acids, whereas the unsaturated fatty acids showed poor oxidation stability [87]. Similarly, lower cloud and pour points were observed in saturated fatty acids, which are higher for unsaturated fatty acids [43]. The result revealed that the primary saturated fatty acids are palmitic (25.7 %) and stearic (11.79 %) for Tucuma biodiesel. Also, the significant unsaturated fatty acid esters are oleic (44.8 %) and octadecadienoic (12.6 %). These four major FAME compositions account for 95 % of Tucuma biodiesel esters. For Ungurahui, oleic (52.11 %), palmitic (23.80 %), linoleic (10.64 %), and stearic (9.60 %) are the significant components in its biodiesel composition, which accounts for 96.15 % of the total composition. Fig. 12 shows the typical chromatogram of Tucuma and Ungurahui oil biodiesel methyl esters for trial 2, representing methyl ester peaks at respective retention times.

3.6. Physiochemical properties of biodiesel

Table 5 compares the physiochemical properties of the Tucuma and Ungurahui biodiesel. The fuel property tests were conducted based on the respective ASTM standards which is presented in Table 5. The study found that the density of 879.1 kg/m^3 (Tucuma) and 880.3 kg/m^3(Ungurahui) are higher than the diesel 832 kg/m^3. The similar results are reported by Ogunkunle and Ahmed [88] and Shalfoh et al. [89]. For both methyl esters, the viscosity is recorded as 4.0 mm^2/s, which is slightly lower and very close to the diesel fuel 4.1 mm^2/s. However, few other methyl esters such as Macadamia (4.46 mm^2/s) and waste cooking oil (4.82) reported by Nabi and Rasul [90] showed higher viscosities. Higher viscosities of the methyl esters will cause problems during the injection period leading to injector choking and piston ring sticking. The

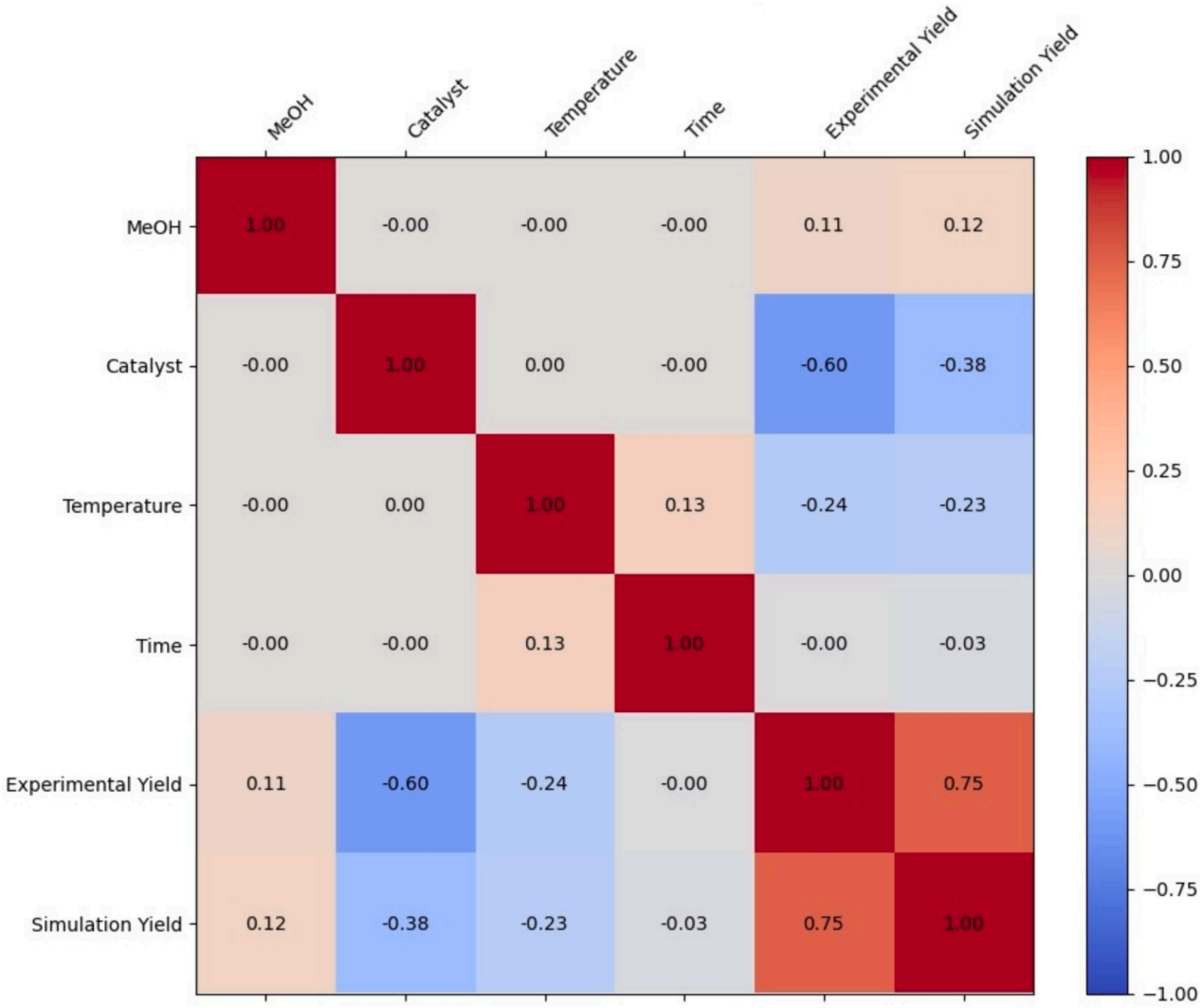

Fig. 14. Correlation matrix heatmap illustrating the strength and direction of correlations between MeOH, catalyst, temperature, and time for experimental and simulation yield.

calorific value for biodiesels (Tucuma:39.87 MJ/kg and Ungurahui:39.82 MJ/kg) is less than the diesel (45.7 MJ/kg). However, the calorific value is closely matched with the biodiesel fuels such as Soybean oil (39.76 MJ/kg), Safflower oil (38.12 MJ/kg), and Peanut oil (40.1 MJ/kg) reported by [91]. The higher density and lower calorific value of the fuels will lead to lower brake power and higher fuel consumption [92,93]. Higher flash points and lower cloud points are observed for Tucuma and Ungurahui biodiesel fuels compared to diesel.

4. Biodiesel simulation results to analyse the effect of process parameters

4.1. Validation of simulated yield by the experimental results

Fig. 13 presents a comparison of simulation and experimental yield results from 27 conducted tests (tests as mentioned in Table 2). Except for test runs 7 and 14, all experimental and simulation results exhibited below 5 % errors. The difference in errors is due to the systematic errors involved in the process. As described in the methodology section, the experimental tests involved continuous transfer of fluids from a conical flask to a three-neck flask, then to a separatory funnel, and finally to a beaker. Various processes, such as transesterification reaction, glycerol separation, water washing, and FAME purification, were conducted between these transfer stages. Given the complexity of these procedures and the potential for both system and manual errors, slight variations between simulation and experimental results are expected. Overall, the experimental and simulation results are in good agreement and further properties analysis was conducted from the simulation results.

4.2. Sensitivity analysis

Fig. 14 illustrates the correlation of the conversion parameters on the simulation and experimental yield parameters. The correlation matrix heatmap visually represents the relationships between process variables: MeOH, catalyst, temperature and time. From the Fig. 14 it is observed that MeOH and catalyst exhibits near-zero correlations with all other input variables, suggesting that MeOH and catalyst levels do not have interdependency with the other factors in this study. The catalyst shows a strong negative correlation with both experimental yield (−0.60) and simulation yield (−0.38), indicating that as the amount of catalyst increases, both the experimental and simulation yields tend to decrease. Additionally, temperature has also showed negative correlations with experimental (−0.24) and simulation data (−0.23), suggesting that higher temperatures may slightly reduce yields. It is to be noted that these correlations are based on the overall behaviours across the specific operating ranges of the other variables. As per the sensitivity analysis, it

Table 6
Physio-chemical properties of the pure methyl esters.

FAME	Density (kg/m^3) at 15 °C	Viscosity (mm^2/s) at 40 °C	Calorific value (MJ/kg) [96]
Methyl Oleate	877.4 [97]	3.93 [97]	41
Methyl Palmitate	866.49 [98]	4.2 [99]	41
Methyl Stearate	855 [100]	5.85 [100]	36
Methyl Linoleate	889.9 [97]	3.22 [97]	35

is evident that the catalyst and temperatures are critical factors inversely affecting both experimental and simulation yields. The weak correlations involving time suggest this variable may not be as influential in this context. The strong correlation between experimental and simulation yields supports the reliability of the simulation model.

4.3. Effect of process parameters on biodiesel physical properties

Biodiesel is chemically simple, which is the combination of a few fatty acids, and the physiochemical behaviour of the biodiesel depends on the FAME. To investigate the impact of process parameters on individual methyl ester components, model simulations were conducted to observe the conversion rates at the molecular level. From the GCMS tests, it is predicted that methyl esters such as methyl oleate, methyl palmitate, methyl stearate, and methyl linoleate were major components in the Tucuma. As mentioned earlier, POO, POP, and OOO, PLS, PPP, PLL, PLP, POS, SLL, SOO and SLO were used as the Tucuma bio-oil as the input to the simulation. The simulation output is the individua pure methyl esters such as methyl oleate, methyl palmitate, methyl stearate, and methyl linoleate. The physicochemical properties of these pure methyl esters of Tucuma oil are presented in Table 6. The conversion rates and the properties of the total biodiesel from simulation is calculated based on the values presented in Table 6. As per the composition of the methyl esters obtained the simulation, the properties of the overall mixture were calculated. The following sections illustrate the impact of individual methyl esters and their compositional variations with the biodiesel process parameters.

4.3.1. Effect of process parameters on biodiesel methyl esters

Fig. 15 illustrates the effect of Tucuma oil methyl esters on methanol concentration and time. As the methanol to oil molar ratio increases from 5:1 to 6:1, both methyl oleate and methyl linoleate initially

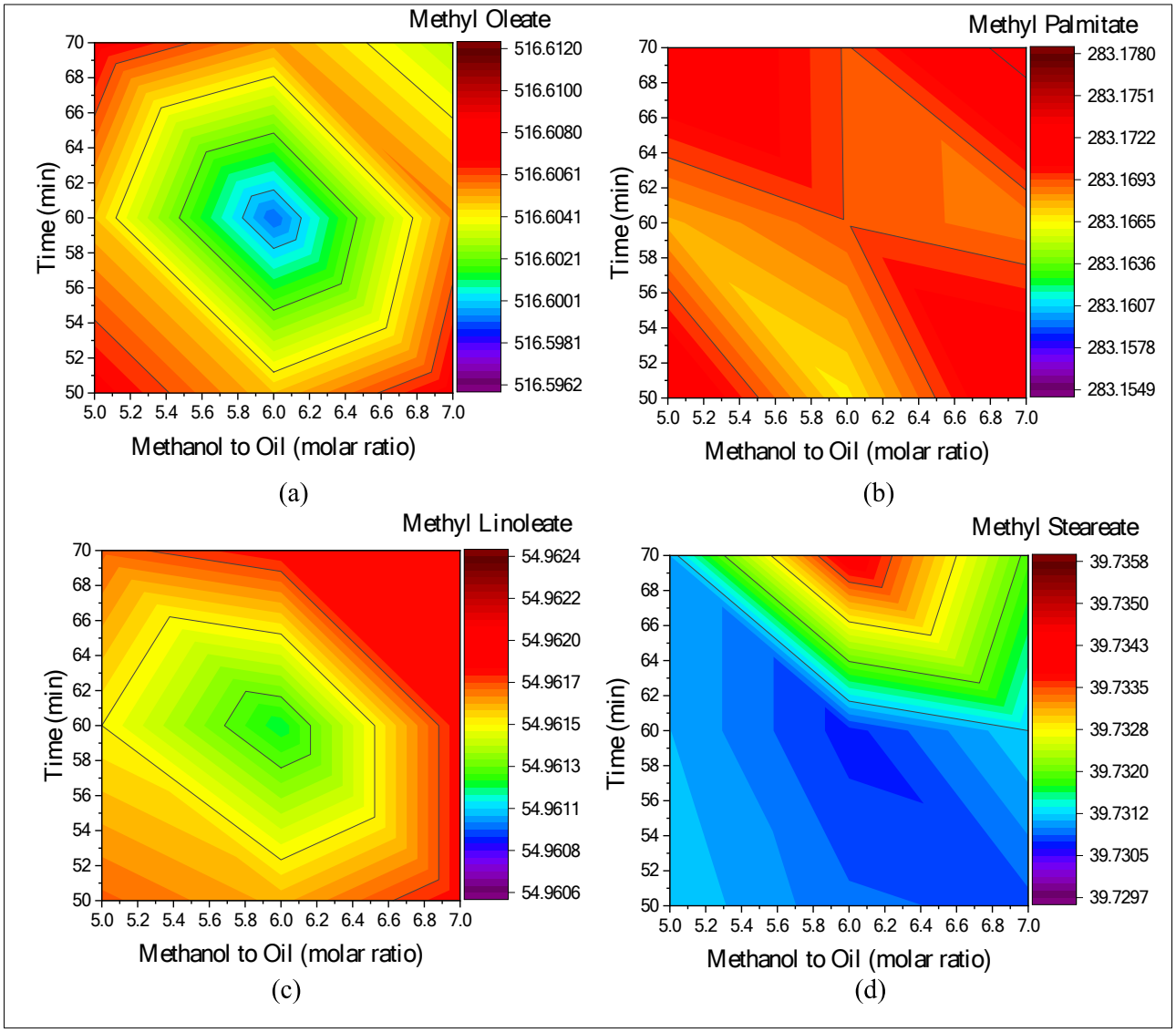

Fig. 15. Effect of Methanol to oil molar ratio and time conditions on (a) methyl oleate; (b) methyl palmitate; (c) methyl linoleate; (d) methyl stearate.

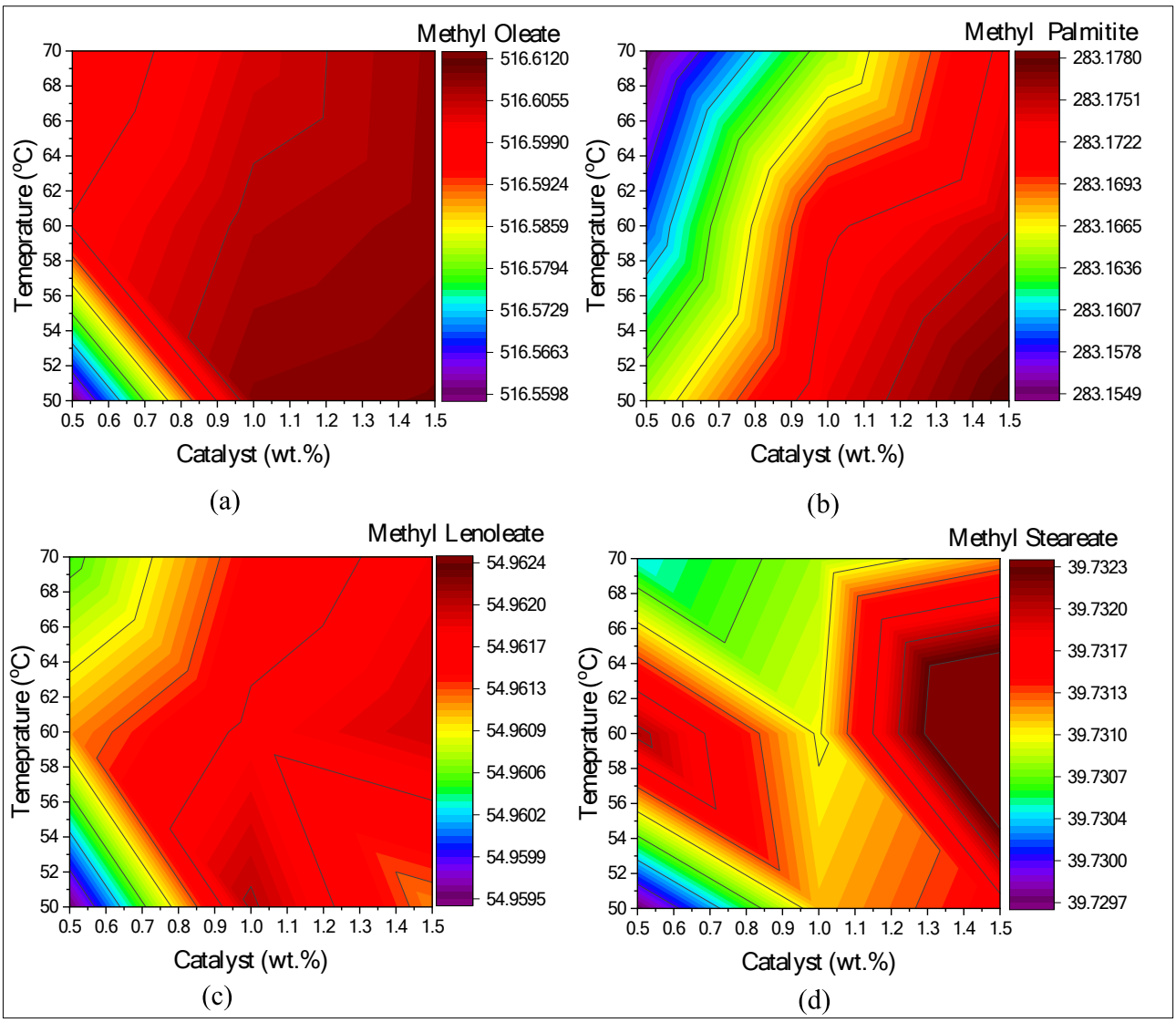

Fig. 16. Effect of catalyst and temperature conditions on (a) methyl oleate; (b) methyl palmitate; (c) methyl linoleate; (d) methyl stearate.

decrease and then increase with further increments to 7:1. This trend is also observed with respect to the time parameter. This could be due to the excess methanol likely shifts the equilibrium towards ester formation, resulting in increased concentrations of these methyl oleate and linoleate. Methyl palmitate conversion rates show less sensitivity to variations in process parameters such as methanol and time. This could be due to better solubility of methyl palmitate in methanol. On the contrary, time emerges as the most influential parameter for methyl stearate. Higher concentrations of stearate were observed at a duration of 70 min. Specifically, at 70 min, methyl stearate increases with an increase in the molar ratio from 5:1 to 6:1 but then decreases with further increments to 7:1. The initial increase from 5:1 to 6:1 in the molar ratio of methanol likely provides a more favourable environment for the reaction to progress, enhancing the formation of methyl stearate. However, at a 7:1 ratio, the excess methanol may again lead to a dilution effect, reducing the rate of methyl stearate formation despite the longer reaction time [101,102].

Fig. 16 describes the effect of catalyst and temperature conditions on the different methyl esters. From experimental ANOVA analysis, it is clearly evident that temperature and catalyst are the primary factors affecting biodiesel conversion rates. Both temperature and catalyst clearly have an impact on the overall conversion. The increase in temperature has led to higher conversion rates of methyl oleate. However, for stearate and linoleate, the conversion initially increased from 50 °C to 60 °C but then decreased as the temperature was raised to 70 °C. This could be due to the equilibrium shift of stearate and linoleate reactants with the increase in temperatures. In contrast, the conversion of methyl palmitate showed higher levels of reaction near 50 °C. The catalyst composition showed noticeable changes as its quantity increased in the reactions. The conversion rates of all methyl esters increased with higher percentages of the catalyst. Similar results are also noticed in the literature Welter et al. [103], Nandiwale and Bokade [104] and Brakora et al. [105].

4.3.2. *Effect of process parameters on biodiesel calorific value*

The effect of transesterification operating conditions on the biodiesel calorific value is shown in Fig. 17(a), where the biodiesel calorific value increases with the increase in the methanol-to-oil molar ratio in the transesterification reaction. Moreover, the calorific value increases with increasing catalyst concentration in the reaction process. The calorific value is lower for the biodiesel obtained from higher reaction temperatures. As shown in Fig. 17(b), a higher calorific value is noted at 50 °C across all molar ratio concentrations. However, at 70 °C and a molar ratio of 7:1, a slightly higher calorific value is noticed compared to the value at 70 °C and with a molar ratio of 6:1. This could be due to presence of fewer unreacted triglycerides, often these reduces the

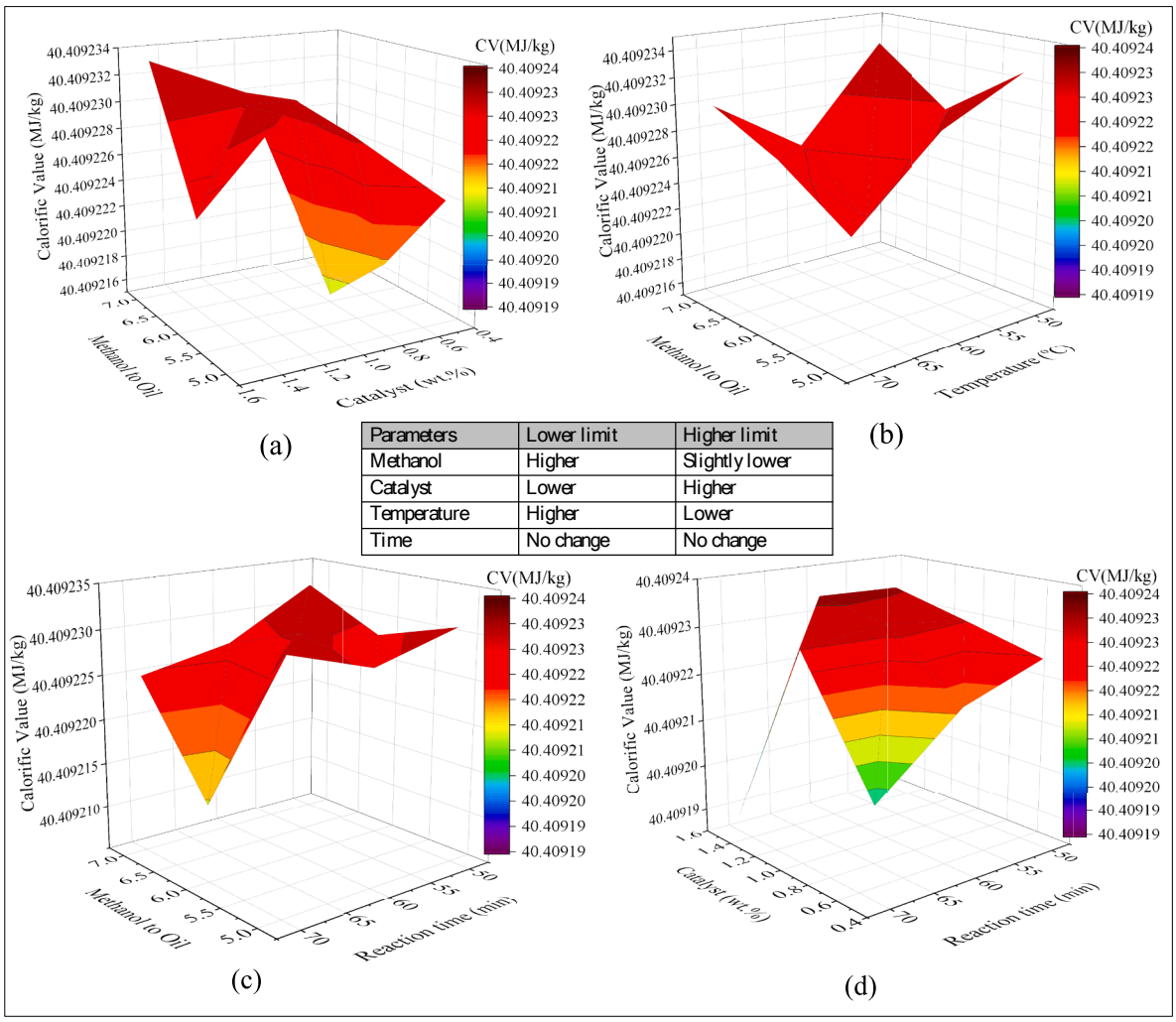

Fig. 17. Effect of process parameters on calorific value: (a) MEOH and catalyst; (b) MEOH and temperature; (c) MEOH and time; (d) catalyst and temperature.

calorific value of the fuel [106]. From Fig. 17(c), it is observed that a higher calorific value is noticed for all molar ratios (5:1, 6:1, and 7:1) at 50 min and 60 min of reaction time periods. However, at 70 min, higher calorific values are noticed at the lower molar ratio of 5:1, and with increasing molar ratio, a reduction in the heating value is noticed. As shown in Fig. 17(d), the higher calorific value is noticed under higher temperatures and lower catalyst reaction conditions. At the same time, a higher heating value is noticed under lower temperatures and higher catalyst concentration reaction conditions. Lower catalyst concentrations at higher temperatures hinders the reaction, preventing the reduction of esters and maintaining the biodiesel's energy content [107].

4.3.3. *Effect of process parameters on biodiesel density*

From Fig. 18(a), it is observed that methyl esters with lower density are obtained under higher catalyst concentration conditions, whereas an increase in density is observed with decreasing catalyst concentrations. Moreover, lower density regions are noticed near a 6:1 methanol ratio even at lower catalyst concentrations, but at a 7:1 ratio and 0.5 wt% catalyst condition, higher density methyl esters were noticed. This behaviour indicating that too much methanol can lead to incomplete or inefficient reactions, possibly due to excess reactants diluting the catalyst's effectiveness. As shown in Fig. 18(b), low-density methyl esters were formed near regions of low reaction temperature. With an increase in temperature, higher density concentrations were observed. This is due to the formation of triglycerides again at higher temperatures due to equilibrium shift and increases the density [108]. Lower-density methyl esters were noticed at methanol molar ratios between 5:1 and 7:1 and reaction temperatures. With an increase in reaction temperature to 70 °C, the density of methyl esters increased. From Fig. 18(c), it is observed that lower reaction times have created higher-density esters at the 6:1 M ratio condition. A decrease in ester density was noticed with an increase in reaction time. From Fig. 18(d), it is noticed that under both lower temperature and higher catalyst concentration conditions, low-density methyl esters were formed. Even at higher temperatures, a higher weight percentage of catalyst has shown its effect and showed less dense methyl ester formation. Besides, higher density is noticed at lower catalyst weight percentages and high-temperature conditions.

4.3.4. *Effect of process parameters on biodiesel viscosity*

Fig. 19(a) depicts that Lower viscosity esters were noticed near the 5:1 and 7:1 methanol-to-oil molar ratio conditions. However, at a 6:1 ratio, higher viscosity is noticed. This could be due to the formation of intermediate or partially reacted compounds, leading to a higher overall viscosity. Moreover, regions with 1.5 wt% catalyst showed the formation of esters with higher viscosities. The main reason behind this is higher catalyst concentrations produces denser side products that can increase the ester viscosity [109]. As shown in Fig. 19(b), at higher reaction temperatures, the viscosity of the generated biodiesel yield was very low. At lower temperatures, esters with higher viscosities were noticed, but only at lower molar ratio concentrations. At higher molar ratios (7:1) and lower temperatures (50 °C and 60 °C), lower viscosity

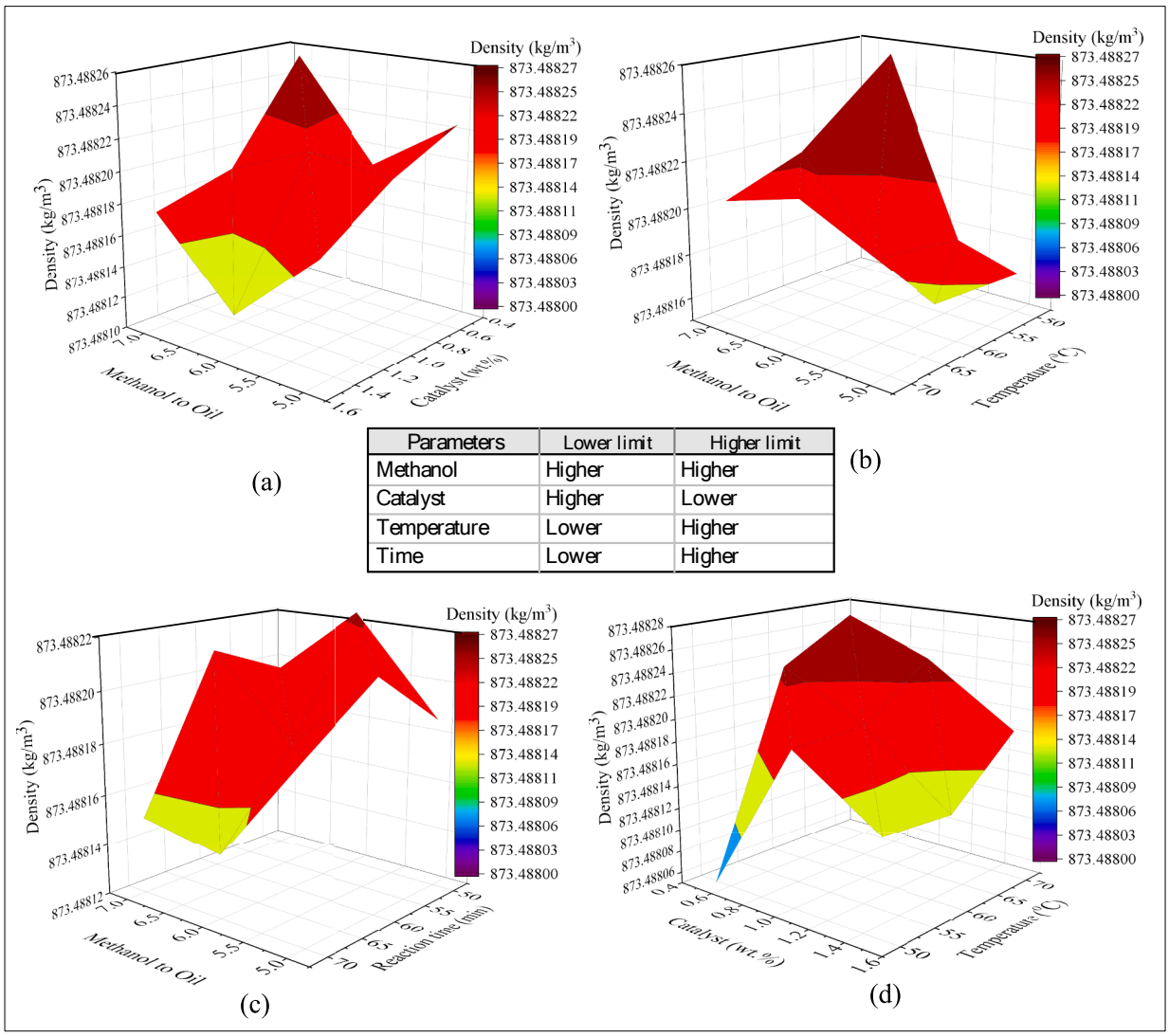

Parameters	Lower limit	Higher limit
Methanol	Higher	Higher
Catalyst	Higher	Lower
Temperature	Lower	Higher
Time	Lower	Higher

Fig. 18. Effect of process parameters on density; (a) Methanol to oil molar ratio and catalyst; (b) Methanol to oil molar ratio and temperature; (c) Methanol to oil molar ratio and time; (d) catalyst and temperature.

esters were noticed. From Fig. 19(c), it is observed that the viscosity of the esters increased with an increase in the molar ratio up to 6:1 and then decreased with a further rise to 7:1. Excess methanol helps in completing the reaction and reducing the presence of intermediate and can reduce the viscosity [110]. Lower viscosity values are noted at 50 min and 60 min time intervals, but at 70 min, high viscosity esters were formed. Fig. 19(d) illustrates that higher viscosities are noticed at lower temperatures (50 °C), particularly at lower catalyst concentrations (0.5 wt%), then decrease at 1.0 wt%, and increase again at 1.5 wt%. However, as mentioned earlier, higher temperatures have reduced the viscosity across all catalyst ranges. Overall, achieving low-viscosity biodiesel involves carefully optimizing the transesterification conditions, including the methanol-to-oil molar ratio, catalyst concentration, reaction temperature, and reaction time [111,109].

5. Influence of this study for practical applications

Tucuma and Ungurahui have shown higher yield conversion results, and based on their physiochemical properties, they are suitable for biodiesel commercialization. The conversion statistics of FFA to FAME indicated that temperature and catalyst concentrations are sensitive parameters affecting biodiesel yield. Similar behaviour is also reported with feedstocks such as WCO [112], Jatropha [113] and Dairy Washed Milk Scum [114]. In contrast, catalyst concentration has less influence on feedstocks like rubber seed oil and flax seed oil [115] during their biodiesel conversion process. On the other hand, reaction time and methanol to oil molar ratio affect the yield but not as much as the temperature and catalyst. This trend is also supported by the feedstocks WCO [112], Jatropha [113] and Dairy Washed Milk Scum [114]. However, feedstocks such as castor oil [116], Pongamia [117] and mealworm [118] has showed sensible interactions with the time and methanol to oil molar ratio parameters. There were number of biodiesel feedstocks that matches the ASTM or EU standards and yet researchers are facing trouble with the same fuels in terms of combustion aspects. This is because of higher densities and lower calorific values [119,120].

One thing is clear that, the chemical structure of one feedstock is fixed, and while its composition cannot be changed, the composition of the fuel can be altered by various means. For instance, majority of the reported biodiesel feedstocks contains free fatty acids such as Oleic, Palmitic, Lauric, Stearic, linoleic, Myristic and few others which will be varied in various proportions with respect to the feedstock [121–123]. Most importantly, each long-chain fatty acid requires different reaction kinetics to gain its kinetic energy for the conversion of respective methyl ester. The simulation study enabled to investigate the effect of the biodiesel conversion parameters of the individual methyl ester components. Irrespective of the feedstock, one can understand the behaviour of the

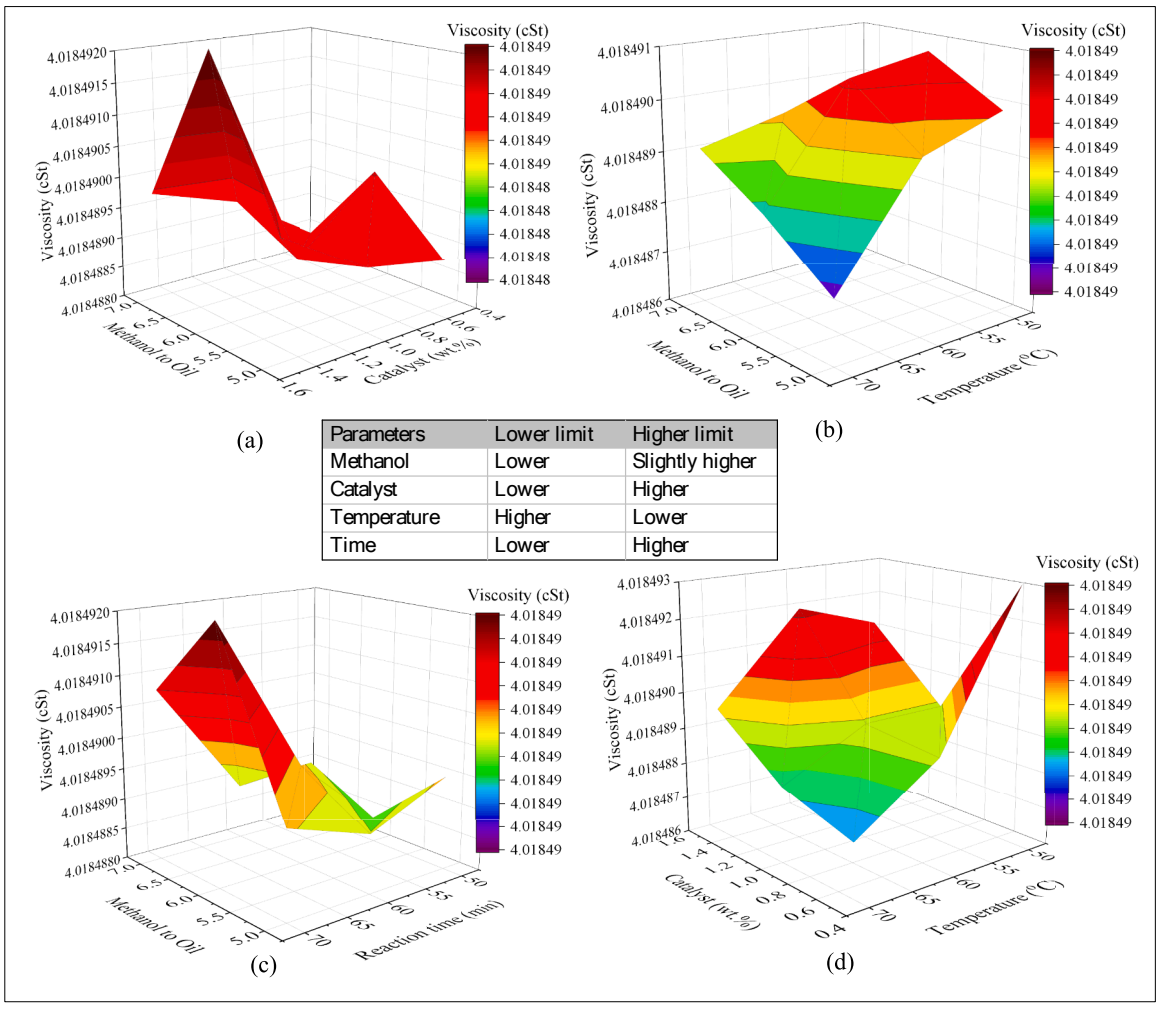

Parameters	Lower limit	Higher limit
Methanol	Lower	Slightly higher
Catalyst	Lower	Higher
Temperature	Higher	Lower
Time	Lower	Higher

Fig. 19. Effect of process parameters on viscosity; (a) MEOH and catalyst; (b) MEOH and temperature; (c) MEOH and time; (d) catalyst and temperature.

conversion process. For instance, as per the simulation, longer time is needed for the conversion of linoleic to the methyl linoleate. Rashid et al. [124] observed higher yield of sunflower biodiesel at longer time periods because sunflower has the higher linoleic content (64 % by weight) in its total composition. In addition, canola oil with high oleic content, showed reduced yield at higher temperatures [125], which is also supporting the simulation outcome, where methyl oleate conversions occurred at lower temperatures. Hence as per the composition of the feedstocks the process parameters can be regulated for the better yield. Moreover, these variations are beneficial in estimating the physio chemical properties of the overall composition based on the feedstock composition.

6. Conclusion and recommendations

The study investigated the impact of biodiesel production parameters on yield. Through statistical optimization, the most influential parameters methanol molar ratio (5:1, 6:1, and 7:1), catalyst concentration (0.5 wt%, 1 wt%, and 1.5 wt%), reaction time (50 min, 60 min, and 70 min), and reaction temperature (50 °C, 60 °C, and 70 °C) were applied to the transesterification process for Tucuma and Ungurahui biodiesel conversion. The conclusions drawn from the study are as follows:

1. The ANOVA analysis indicates that catalyst concentration has a highly significant impact on yield conversion (p-value of 0.0 for both biodiesels). Temperature also significantly affects yield (p-values < 0.05). In contrast, methanol and time have higher p-values, suggesting they have less influence on yield conversion.
2. At the optimized condition a higher yield of 99.4 % ± 0.2 % and 99.2 % ± 0.4 % was observed for Tucuma and Ungurahui, respectively.
3. Viscosity for both fuels is recorded as 4.0 mm^2/s which is lower than the diesel fuel 4.1 mm^2/s, which makes them more suitable for the direct injection engines. However, the calorific value of both fuels is low compared to diesel.
4. Tucuma biodiesel transesterification was modelled in Aspen plus and simulation yield results are validated with 27 experimental yield results. The test results were satisfactorily valid and among them 25 test results were less than 5 % error margin.
5. Catalyst and temperature have affected the conversion rates of Methyl oleate, Methyl Palmitate, and Methyl linoleate, whereas methyl stearate was affected by the time parameters. Thus, in practical applications, the biodiesel process parameters can be varied based on their feedstock's fatty acid composition.
6. A higher calorific value was recorded under low temperature and methanol-to-oil molar ratio conditions, while lower density esters were observed at low temperature and shorter reaction time conditions. Additionally, lower viscosity esters were noticed under conditions of lower methanol, lower catalyst concentration, and shorter reaction time. Although the variation in properties is small in lab-scale experiments, these differences can significantly impact commercial-scale production applications.

The study recommends that both Tucuma and Ungurahui show promising potential as feedstocks for biodiesel conversion. Considering the high market value of Tucuma and Ungurahui oils the study recommends exploring the potential for their cultivation in an economically feasible manner to support their use in biodiesel production. Additionally, future studies should focus on developing and integrating effective wastewater management and disposal strategies to address the environmental challenges associated with the transesterification process using potassium hydroxide as a catalyst. These efforts will contribute to the overall sustainability and economic viability of biodiesel production from these oils. Furthermore, the study suggests conducting experimental investigations by deploying these biodiesels into a diesel engine on both fuels to analyze their performance, combustion characteristics, and emission behavior before recommending them for commercial application.

CRediT authorship contribution statement

Arun Teja Doppalapudi: Writing – original draft, Visualization, Validation, Software, Methodology, Formal analysis, Data curation, Investigation, Conceptualization. **Abul Kalam Azad:** Writing – review & editing, Visualization, Validation, Supervision, Software, Resources, Project administration, Methodology, Investigation, Conceptualization. **M.M.K. Khan:** Writing – review & editing, Supervision, Resources, Conceptualization. **Amanullah Maung Than Oo:** .

Declaration of competing interest

The authors declare that they have no known competing financial interests or personal relationships that could have appeared to influence the work reported in this paper.

Data availability

Data will be made available on request.

Acknowledgements

The authors would like to express our heartfelt gratitude to Senior Engineers Mr. Naveen Murugan, Ms. Mahdieh Azimi Adeh Morteza Pasha, and Mr. Michael Vernon for their invaluable assistance in conducting the optimization simulation in the CQU Melbourne campus laboratory. The authors are also deeply thankful to Ms. Tania Collins and her team from CQUniversity, School of Health, Medical and Applied Sciences for their support in performing GC-MS tests for the prepared biodiesel.

Appendix A. Supplementary data

Supplementary data to this article can be found online at https://doi.org/10.1016/j.ecmx.2024.100721.

References

[1] Reza Talaghat, M, Mokhtari S, Saadat M. Modeling and optimization of biodiesel production from microalgae in a batch reactor. Fuel 2020;280:118578.
[2] Sawarkar AN. Reaction kinetics and coke forming propensities of Arabian mix asphalt vis-a-vis Arabian mix vacuum residue. Pet Sci Technol 2022;40(11):1333–48.
[3] Omid MA, Şahin ME, Cora ÖN. Challenges and future perspectives on production, storage technologies, and transportation of hydrogen: a review. Energ Technol 2024;12(4):2300997.
[4] Soudagar MEM, Shelare S, Marghade D, Belkhode P, Nur-E-Alam M, Kiong TS, et al. Optimizing IC engine efficiency: a comprehensive review on biodiesel, nanofluid, and the role of artificial intelligence and machine learning. Energy Convers Manage 202;307:118337.
[5] Ağbulut Ü. Forecasting of transportation-related energy demand and CO2 emissions in Turkey with different machine learning algorithms. Sustain Prod Consumpt 2022;29:141–57.
[6] Chisti Y. Biodiesel from microalgae. Biotechnol Adv 2007;25(3):294–306.
[7] Deshpande G, Shrikhande S, Sawarkar AN, Patle DS. Multiobjective optimization of ultrasound intensified and ionic liquid catalyzed in situ algal biodiesel production considering economic, environmental and safety indicators. Chem Eng Res Des 2022;180:134–52.
[8] Sarıdemir S, Polat F, Ağbulut Ü. Improvement of worsened diesel and waste biodiesel fuelled-engine characteristics with hydrogen enrichment: a deep discussion on combustion, performance, and emission analyses. Process Saf Environ Prot 2024;184:637–49.
[9] Al-Mawali KS, Osman AI, Al-Muhtaseb AaH, Mehta N, Jamil F, Mjalli F, et al. Life cycle assessment of biodiesel production utilising waste date seed oil and a novel magnetic catalyst: a circular bioeconomy approach. Renew Energy 2021;**170**: p. 832-846.
[10] IEA. Renewables 2023, IEA; 2023. Available from: https://www.iea.org/reports/renewables-2023.
[11] Fonseca C, Jiang H, Zeerak R, Zhao JZ. Explaining the adoption of electric vehicle fees across the United States. Transp Policy 2024;149:139–49.
[12] Mittal G, Garg A, Pareek K. A review of the technologies, challenges and policies implications of electric vehicles and their future development in India. Energy Storage 2024;6(1):e562.
[13] Peng R, Tang JHCG, Yang X, Meng M, Zhang J, Zhuge C. Investigating the factors influencing the electric vehicle market share: a comparative study of the European Union and United States. Appl Energy 2024;355:122327.
[14] Damian CS, Devarajan Y, Jayabal R. Biodiesel production in India: prospects, challenges, and sustainable directions. Biotechnol Bioeng 2024;121(3):894–902.
[15] Das P, Jha CK, Saxena S, Ghosh RK. Can biofuels help achieve sustainable development goals in India? A systematic review. Renew Sustain Energy Rev 2024;192:114246.
[16] Mayandi Z, Suharjito. Palm oil-based biodiesel industry sustainability model using dynamic systems to balance food, energy, and export allocations. Smart Agric Technol 2024;7:100421.
[17] OECD. OECD-FAO Agricultural Outlook; 2023 [cited 2024].
[18] OECD/FAO. OECD-FAO Agricultural Outlook. OECD Agriculture Statistics; 2022.
[19] Ong HC, Chen W-H, Farooq A, Gan YY, Lee KT, Ashokkumar V. Catalytic thermochemical conversion of biomass for biofuel production: a comprehensive review. Renew Sustain Energy Rev 2019;113:109266.
[20] Saadi W, Rodríguez-Sánchez S, Ruiz B, Souissi-Najar S, Ouederni A, Fuente E. Pyrolysis technologies for pomegranate (Punica granatum L.) peel wastes. Prospects in the bioenergy sector. Renew Energy 2019;136:373–382.
[21] Chong CT, Mong GR, Ng J-H, Chong WWF, Ani FN, Lam SS, et al. Pyrolysis characteristics and kinetic studies of horse manure using thermogravimetric analysis. Energ Conver Manage 2019;180:1260–7.
[22] Lee XJ, Ong HC, Gao W, Ok YS, Chen W-H, Goh BHH, et al. Solid biofuel production from spent coffee ground wastes: Process optimisation, characterisation and kinetic studies. Fuel 2021;292:120309.
[23] Santos PDdF, Batista PS, Torres LCR, Thomazini M, de Alencar SM, Favaro-Trindade CS. Application of spray drying, spray chilling and the combination of both methods to produce tucumã oil microparticles: characterization, stability, and β-carotene bioaccessibility. Food Res Int 2017;2:113174.
[24] Ferreira MJA, Mota MFS, Mariano RGB, Freitas SP. Evaluation of liquid-liquid extraction to reducing the acidity index of the tucuma (Astrocaryum vulgare Mart.) pulp oil. Sep Purif Technol 2021;257:117894.
[25] Cândido TLN, Silva MR, Agostini-Costa TS. Bioactive compounds and antioxidant capacity of buriti (Mauritia flexuosa L.f.) from the Cerrado and Amazon biomes. Food Chem 2015;177:313–319.
[26] Escriche I, Restrepo J, Serra J, Herrera L. Composition and nutritive value of Amazonian palm fruits. Food Nutr Bull 1999;20(3):361–5.
[27] Jaramillo-Vivanco T, Balslev H, Montúfar R, Cámara RM, Giampieri F, Battino M, et al. Three Amazonian palms as underestimated and little-known sources of nutrients, bioactive compounds and edible insects. Food Chem 2022;372:131273.
[28] Ter Steege H, Pitman NC, Sabatier D, Baraloto C, Salomão RP, Guevara JE, et al. Hyperdominance in the Amazonian tree flora. Science 2013;342(6156):1243092.
[29] de Freitas FA, Mendonça IRS, Barros SdS, Pessoa Jr WGA, Sá ISC, Gato LB, et al. Biodiesel production from tucumã (Astrocaryum aculeatum Meyer) almond oil applying the electrolytic paste of spent batteries as a catalyst. Renew Energy 2022;191:919–931.
[30] Moyo LB, Iyuke SE, Muvhiiwa RF, Simate GS, Hlabangana N. Application of response surface methodology for optimization of biodiesel production parameters from waste cooking oil using a membrane reactor. S Afr J Chem Eng 2021;35:1–7.
[31] Azad AK, Jadeja AC, Doppalapudi AT, Hassan NM, Nabi MN, Rauniyar R. Design and simulation of the biodiesel process plant for sustainable fuel production. Sustainability 2024;16. DOI: 10.3390/su16083291.
[32] Doppalapudi AT, Azad AK. Advanced numerical analysis of in-cylinder combustion and NOx formation using different chamber geometries. Fire 2024;7. DOI: 10.3390/fire7020035.
[33] Doppalapudi AT, Azad AK, Khan MMK. Combustion chamber modifications to improve diesel engine performance and reduce emissions: a review. Renew Sustain Energy Rev 2021;152:111683.
[34] Selvaraj R, Moorthy IG, Kumar RV, Sivasubramanian V. Microwave mediated production of FAME from waste cooking oil: Modelling and optimization of process parameters by RSM and ANN approach. Fuel 2019;237:40–9.
[35] Ashok B, Nanthagopal K, Saravanan B, Azad K, Patel D, Sudarshan B, et al. Study on isobutanol and Calophyllum inophyllum biodiesel as a partial replacement in CI engine applications. Fuel 2019;235:984–994.

[36] Doppalapudi AT, Azad AK, Khan MM. Analysis of improved in-cylinder combustion characteristics with chamber modifications of the diesel engine. Energies 2023;16. DOI: 10.3390/en16062586.
[37] Lugo-Méndez H, Sánchez-Domínguez M, Sales-Cruz M, Olivares-Hernández R, Lugo-Leyte R, Torres-Aldaco A. Synthesis of biodiesel from coconut oil and characterization of its blends. Fuel 2021;295:120595.
[38] Doppalapudi AT, Azad AK, Khan MMK. Advanced strategies to reduce harmful nitrogen-oxide emissions from biodiesel fueled engine. Renew Sustain Energy Rev 2023;174:113123.
[39] Lanjekar RD, Deshmukh D. A review of the effect of the composition of biodiesel on NOx emission, oxidative stability and cold flow properties. Renew Sustain Energy Rev 2016;54:1401–11.
[40] Ramírez-Verduzco LF, Rodríguez-Rodríguez JE, Jaramillo-Jacob AdR. Predicting cetane number, kinematic viscosity, density and higher heating value of biodiesel from its fatty acid methyl ester composition. Fuel 2012;91(1):102–111.
[41] Satyanarayana M, Muraleedharan C. A comparative study of vegetable oil methyl esters (biodiesels). Energy 2011;36(4):2129–37.
[42] Bukkarapu KR, Krishnasamy A. A study on the effects of compositional variations of biodiesel fuel on its physiochemical properties. Biofuels 2021;12(5):523–35.
[43] Knothe G. "Designer" biodiesel: optimizing fatty ester composition to improve fuel properties. Energy Fuel 2008;22(2):1358–64.
[44] Azad AK, Rasul MG, Khan MMK, Sharma SC, Islam R. Prospect of moringa seed oil as a sustainable biodiesel fuel in australia: a review. Proc Eng 2015;105:601–6.
[45] Bhuiya MMK, Rasul MG, Khan MMK, Ashwath N, Azad AK, Hazrat MA. Second generation biodiesel: potential alternative to-edible oil-derived biodiesel. Energy Proc 2014;61:1969–72.
[46] Azad AK, Doppalapudi AT, Khan MMK, Hassan NMS, Gudimetla P. A landscape review on biodiesel combustion strategies to reduce emission. Energy Rep 2023;9:4413–36.
[47] Santos MdFGd, Alves RE, Brito ESD, Silva SDM, Silveira MRSD. Quality characteristis of fruits and oils of palms native to the brazilian amazon. Revista Brasileira de Fruticultura 2017;39.
[48] Kefale Mangesha Y, Nallamothu RB, Ancha VR, Tesfaye Tefera N. Optimization, production, and characterization of cottonseed methyl ester based on Box-Behnken in response surface design and gas chromatography-mass spectrum analysis. Energy Convers Manage: X 2024;23:100619.
[49] Maran JP, Priya B. Comparison of response surface methodology and artificial neural network approach towards efficient ultrasound-assisted biodiesel production from muskmelon oil. Ultrason Sonochem 2015;23:192–200.
[50] Prakash Maran J, Manikandan S. Response surface modeling and optimization of process parameters for aqueous extraction of pigments from prickly pear (Opuntia ficus-indica) fruit. Dyes Pigments 2012;95(3):465–472.
[51] Singh V, Belova L, Singh B, Sharma YC. Biodiesel production using a novel heterogeneous catalyst, magnesium zirconate (Mg2Zr5O12): process optimization through response surface methodology (RSM). Energ Conver Manage 2018;174:198–207.
[52] Azad AK. Biodiesel from mandarin seed oil: a surprising source of alternative fuel. Energies 2017;10. https://doi.org/10.3390/en10111689.
[53] Yaakob Z, Mohammad M, Alherbawi M, Alam Z, Sopian K. Overview of the production of biodiesel from Waste cooking oil. Renew Sustain Energy Rev 2013;18:184–93.
[54] Teles M, Morgavi P, Carrillo Le Roux G. Exploring amazonian fats and oils blends by computational predictions of solid fat content. OCL 2018:25.
[55] Deshpande G, Shrikhande S, Patle DS, Sawarkar AN. Simultaneous optimization of economic, environmental and safety criteria for algal biodiesel process retrofitted using dividing wall column and multistage vapor recompression. Process Saf Environ Prot 2022;164:1–14.
[56] Rabelo G, Andrade M. Simulation and optimization of CSTR reactor of a biodiesel plant by various plant sources using Aspen Plus. Int J Chem React Eng 2020:1.
[57] Giwa A, Giwa S, Olugbade EA. Application of Aspen HYSYS process simulator in green energy revolution: a case study of biodiesel production. J Eng Appl Sci 2018;13:569–81.
[58] Lima Silva N, Wolf Maciel M, Batistella C, Maciel Filho R. Kinetics parameters of castor oil and soybean oil. In Proceedings of the 29th Symposium on Biotechnology for Fuel and Chemicals; 2007.
[59] Silva GCR, Andrade MHC. Development and simulation of a new oil extraction process from fruit of macauba palm tree. J Food Process Eng 2013;36(1):134–45.
[60] Al-Bawwat AaK, Gomaa MR, Cano A, Jurado F, Alsbou EM. Extraction and characterization of Cucumis melon seeds (Muskmelon seed oil) biodiesel and studying its blends impact on performance, combustion, and emission characteristics in an internal combustion engine. Energy Convers Manage: X 2024;23:100637.
[61] Cahyo Kumoro A, Saeed MTMN. Ultrasound-assisted transesterification of tropical goat fat – palm oil blend for biodiesel synthesis. Energy Conversion and Management: X 2022;14:100213.
[62] Ishola NB, Epelle EI, Betiku E. Machine learning approaches to modeling and optimization of biodiesel production systems: state of art and future outlook. Energy Convers Manage: X 2024;23:100669.
[63] Ali MM, Gheni SA, Ahmed SMR, Hmood HM, Hassan AA, Mohammed HR, et al. Catalytic production of biodiesel from waste cooking oil in a two-phase oscillatory baffled reactor: deactivation kinetics and ANN modeling study. Energy Convers Manage: X 2023;19:100383.
[64] Musa IA. The effects of alcohol to oil molar ratios and the type of alcohol on biodiesel production using transesterification process. Egypt J Pet 2016;25(1):21–31.
[65] Saeed A, Hanif M, Haq Nawaz R. The production of biodiesel from plum waste oil using nano-structured catalyst loaded into supports. Sci Rep 2021;11:24120.
[66] Okechukwu OD, Joseph E, Nonso UC, Kenechi N-O. Improving heterogeneous catalysis for biodiesel production process. Clean Chem Eng 2022;3:100038.
[67] Hoque ME, Singh A, Chuan YL. Biodiesel from low cost feedstocks: the effects of process parameters on the biodiesel yield. Biomass Bioenergy 2011;35(4):1582–7.
[68] Wong W-Y, Lim S, Pang Y-L, Shuit S-H, Chen W-H, Lee K-T. Synthesis of renewable heterogeneous acid catalyst from oil palm empty fruit bunch for glycerol-free biodiesel production. Sci Total Environ 2020;727:138534.
[69] Efavi JK, Kanbogtah D, Apalangya V, Nyankson E, Tiburu EK, Dodoo-Arhin D, et al. The effect of NaOH catalyst concentration and extraction time on the yield and properties of Citrullus vulgaris seed oil as a potential biodiesel feed stock. S Afr J Chem Eng 2018;25:98–102.
[70] Jan HA, Osman AI, Al-Fatesh AS, Almutairi G, Surina I, Al-Otaibi RL, et al. Biodiesel production from Sisymbrium irio as a potential novel biomass waste feedstock using homemade titania catalyst. Sci Rep 2023;13(1):11282.
[71] Yameen MZ, AlMohamadi H, Naqvi SR, Noor T, Chen W-H, Amin NAS. Advances in production & activation of marine macroalgae-derived biochar catalyst for sustainable biodiesel production. Fuel 2023;337:127215.
[72] Chouhan APS, Sarma AK. Modern heterogeneous catalysts for biodiesel production: a comprehensive review. Renew Sustain Energy Rev 2011;15(9):4378–99.
[73] Encinar J, Gonzalez J, Rodriguez J, Tejedor A. Biodiesel fuels from vegetable oils: transesterification of Cynara c arduunculus L. oils with ethanol. Energy Fuel 2002;16(2):443–50.
[74] Lingfeng C, Guomin X, Bo X, Guangyuan T. Transesterification of cottonseed oil to biodiesel by using heterogeneous solid basic catalysts. Energy Fuel 2007;21(6):3740–3.
[75] Noiroj K, Intarapong P, Luengnaruemitchai A, Jai-In S. A comparative study of KOH/Al2O3 and KOH/NaY catalysts for biodiesel production via transesterification from palm oil. Renew Energy 2009;34(4):1145–50.
[76] Boz N, Degirmenbasi N, Kalyon DM. Transesterification of canola oil to biodiesel using calcium bentonite functionalized with K compounds. Appl Catal B 2013;138–139:236–42.
[77] Wu X, Leung DYC. Optimization of biodiesel production from camelina oil using orthogonal experiment. Appl Energy 2011;88(11):3615–24.
[78] Nautiyal P, Subramanian K, Dastidar M. Kinetic and thermodynamic studies on biodiesel production from Spirulina platensis algae biomass using single stage extraction–transesterification process. Fuel 2014;135:228–34.
[79] Leung DY, Wu X, Leung MKH. A review on biodiesel production using catalyzed transesterification. Appl Energy 2010;87(4):1083–95.
[80] Agarwal M, Chauhan G, Chaurasia SP, Singh K. Study of catalytic behavior of KOH as homogeneous and heterogeneous catalyst for biodiesel production. J Taiwan Inst Chem Eng 2012;43(1):89–94.
[81] Naik Ramavathu L, Radhika N, Sravani K, Hareesha A, Mohanakumari B, Bhavanasindhu K. Optimized parameters for production of biodiesel from fried oil 2015;2.
[82] Chumuang N, Punsuvon V. Response surface methodology for biodiesel production using calcium methoxide catalyst assisted with tetrahydrofuran as cosolvent. J Chem 2017;2017.
[83] Anwar M, Rasul MG, Ashwath N, Rahman MM. Optimisation of second-generation biodiesel production from Australian native stone fruit oil using response surface method. Energies 2018;11(10):2566.
[84] Weldeslase MG, Benti NE, Desta MA, Mekonnen YS. Maximizing biodiesel production from waste cooking oil with lime-based zinc-doped CaO using response surface methodology. Sci Rep 2023;13(1):4430.
[85] Bhuiya MMK, Rasul MG, Khan MMK, Ashwath N, Azad AK, Hazrat MA. Prospects of 2nd generation biodiesel as a sustainable fuel – Part 2: properties, performance and emission characteristics. Renew Sustain Energy Rev 2016;55:1129–46.
[86] Bibin C, Devan PK, Senthil Kumar S, Gopinath S, Sheeja R. Influence of palmitic and oleic acid mixtures on combustion evaluation of a diesel engine. Mater Today: Proc 2021;45:6638–6644.
[87] Knothe G. Fuel properties of highly polyunsaturated fatty acid methyl esters. Prediction of fuel properties of algal biodiesel. Energy Fuel 2012;26(8):5265–73.
[88] Ogunkunle O, Ahmed NA. Exhaust emissions and engine performance analysis of a marine diesel engine fuelledwith Parinari polyandra biodiesel–diesel blends. Energy Rep 2020;6:2999–3007.
[89] Shalfoh E, Ahmad MI, Binhweel F, Shaah MA, Senusi W, Hossain MS, et al. Fish waste oil extraction using supercritical CO2 extraction for biodiesel production: mathematical, and kinetic modeling. Renew Energy 2024;220:119659.
[90] Nabi MN, Rasul MG. Influence of second generation biodiesel on engine performance, emissions, energy and exergy parameters. Energ Conver Manage 2018;169:326–33.
[91] Mofijur M, Rasul MG, Hyde J, Azad AK, Mamat R, Bhuiya MMK. Role of biofuel and their binary (diesel–biodiesel) and ternary (ethanol–biodiesel–diesel) blends on internal combustion engines emission reduction. Renew Sustain Energy Rev 2016;53:265–78.
[92] Alam M, Song J, Acharya R, Boehman A, Miller K. Combustion and emissions performance of low sulfur, ultra low sulfur and biodiesel blends in a DI diesel engine. SAE Trans 2004:1986–97.
[93] Qi D, Geng L, Chen H, Bian YZ, Liu J, Ren XC. Combustion and performance evaluation of a diesel engine fueled with biodiesel produced from soybean crude oil. Renew Energy 2009;34(12):2706–13.
[94] Knothe G, Razon LF. Biodiesel fuels. Prog Energy Combust Sci 2017;58:36–59.

[95] Azad AK, Halder P, Wu Q, Rasul MG, Hassan NMS, Karthickeyan V. Experimental investigation of ternary biodiesel blends combustion in a diesel engine to reduce emissions. Energy Convers Manage: X 2023;20:100499.
[96] Altaie MAH, Janius RB, Rashid U, Taufiq Yap YH, Yunus R, Zakaria R. Cold flow and fuel properties of methyl oleate and palm-oil methyl ester blends. Fuel 2015;160:238–44.
[97] Pratas MJ, Freitas S, Oliveira MB, Monteiro SC, Lima AS, Coutinho JAP. Densities and viscosities of fatty acid methyl and ethyl esters. J Chem Eng Data 2010;55(9):3983–90.
[98] Altaie MAH, Janius RB, Taufiq-Yap YH, Rashid U. Basic properties of methyl palmitate-diesel blends. Fuel 2017;193:1–6.
[99] Wedler C, Trusler JPM. Review of density and viscosity data of pure fatty acid methyl ester, ethyl ester and butyl ester. Fuel 2023;339:127466.
[100] Soloiu V, Weaver J, Ochieng H, Duggan M, Davoud S, Vlcek B, et al. Experimental study of combustion and emissions characteristics of methyl oleate, as a surrogate for biodiesel, in a direct injection diesel engine. 2013, SAE Technical Paper.
[101] Ahmed RA, Rashid S, Huddersman K. Esterification of stearic acid using novel protonated and crosslinked amidoximated polyacrylonitrile ion exchange fibres. J Ind Eng Chem 2023;119:550–73.
[102] Uzun BB, Kılıç M, Özbay N, Pütün AE, Pütün E. Biodiesel production from waste frying oils: optimization of reaction parameters and determination of fuel properties. Energy 2012;44(1):347–51.
[103] Welter RA, Santana H, de la Torre LG, Robertson M, Taranto OP, Oelgemöller M. Methyl oleate synthesis by TiO2 photocatalytic esterification of oleic acid: optimisation by response surface quadratic methodology, reaction kinetics and thermodynamics. ChemPhotoChem 2022;6(7):e202200007.
[104] Nandiwale KY, Bokade VV. Process optimization by response surface methodology and kinetic modeling for synthesis of methyl oleate biodiesel over H3PW12O40 anchored montmorillonite K10. Ind Eng Chem Res 2014;53(49):18690–8.
[105] Brakora JL, Ra Y, Reitz RD, Combustion model for biodiesel-fueled engine simulations using realistic chemistry and physical properties. SAE Int J Engines 2011;4(1).
[106] Eterigho E, Lee J, Harvey A. Triglyceride cracking for biofuel production using a directly synthesised sulphated zirconia catalyst. Bioresour Technol 2011;102:6313–6.
[107] Mandari V, Devarai SK. Biodiesel production using homogeneous, heterogeneous, and enzyme catalysts via transesterification and esterification reactions: a critical review. Bioenergy Res 2022;15(2):935–61.
[108] Moulita RA, Rusdianasari R, Kalsum L. Converting waste cooking oil into biodiesel using microwaves and high voltage technology. J Phys Conf Ser 2019;1167:012033.
[109] Widayat W, Wibowo A, Hadiyanto H. Study on production process of biodiesel from rubber seed (hevea brasiliensis) by in situ (trans)esterification method with acid catalyst. Energy Proc 2013;32:64–73.
[110] Patel NK, Shah SN. 11 – Biodiesel from Plant Oils. In: Ahuja S, editor. Food, Energy, and Water. Boston: Elsevier; 2015. p. 277–307.
[111] Buchori L, Widayat W, Muraza O, Amali MI, Maulida RW, Prameswari J. Effect of temperature and concentration of zeolite catalysts from geothermal solid waste in biodiesel production from used cooking oil by esterification–transesterification process. Processes 2020;8. doi:10.3390/pr8121629.
[112] Yahya S, Muhamad Wahab SK, Harun FW. Optimization of biodiesel production from waste cooking oil using Fe-Montmorillonite K10 by response surface methodology. Renew Energy 2020;157:164–172.
[113] Lee HV, Yunus R, Juan JC, Taufiq-Yap YH. Process optimization design for jatropha-based biodiesel production using response surface methodology. Fuel Process Technol 2011;92(12):2420–8.
[114] Srikanth HV, Venkatesh J, Godiganur S. Box-Behnken response surface methodology for optimization of process parameters for dairy washed milk scum biodiesel production. Biofuels 2021;12(1):113–23.
[115] Ahmad T, Danish M, Kale P, Geremew B, Adeloju SB, Nizami M, et al. Optimization of process variables for biodiesel production by transesterification of flaxseed oil and produced biodiesel characterizations. Renew Energy 2019;139:1272–80.
[116] Obayomi K, Bello J, Ogundipe T, Olawale O. Extraction of castor oil from castor seed for optimization of biodiesel production. IOP Conf Ser: Earth Environ Sci 2020;445:012055.
[117] Poojary S, Rao CV, Kanthakere S, Shet V. Process optimisation of pilot scale biodiesel production from pongamia and waste cooking oil feedstock. J Eng Sci Technol 2018;13:2670–84.
[118] Siow HS, Sudesh K, Ganesan S. Insect oil to fuel: Optimizing biodiesel production from mealworm (Tenebrio molitor) oil using response surface methodology. Fuel 2024;371:132099.
[119] Doppalapudi AT, Azad AK. Advanced numerical analysis of in-cylinder combustion and NOx formation using different chamber geometries. Fire 2024;7(2):35.
[120] Doppalapudi AT, Azad AK, Khan MMK. Exergy, energy, performance, and combustion analysis for biodiesel NOx reduction using new blends with alcohol, nanoparticle, and essential oil. J Clean Prod 2024;467:142968.
[121] Azad AK, Adhikari J, Halder P, Rasul MG, Hassan NM, Khan MM, et al. Performance, emission and combustion characteristics of a diesel engine powered by macadamia and grapeseed biodiesels. Energies 2020;13(11):2748.
[122] Azad AK, Rasul M, Khan MMK, Sharma SC, Hazrat M. Prospect of biofuels as an alternative transport fuel in Australia. Renew Sustain Energy Rev 2015;43:331–51.
[123] Bhuiya M, Rasul M, Khan M, Ashwath N, Azad A, Hazrat M. Prospects of 2nd generation biodiesel as a sustainable fuel–Part 2: properties, performance and emission characteristics. Renew Sustain Energy Rev 2016;55:1129–46.
[124] Rashid U, Anwar F, Arif M. Optimization of base catalytic methanolysis of sunflower (Helianthus annuus) seed oil for biodiesel production by using response surface methodology. Ind Eng Chem Res 2009;48(4):1719–26.
[125] Sinha A, Jazie AA, Pramanik H. Optimization of biodiesel production from peanut and rapeseed oils using response surface methodology ali. Int J Biomass Renew 2012;1(2):9–18.